

## ABSTRACT

Title of Document: MULTIPLE HRG-1 PARALOGS REGULATE  
HEME HOMEOSTASIS  
IN *C. ELEGANS*.

Haifa Ben Saidan, Master of Science, 2014

Directed By: Professor Iqbal Hamza, Department of Animal  
and Avian sciences

Heme is an essential cofactor for various biological processes although the pathways for cellular heme transport remain poorly understood. We identified HRG-1 as the first *bona fide* eukaryotic heme importer/transporter using *C. elegans*. The current study seeks to determine how HRG-1 paralogs function in heme transport. We show that CeHRG-6 specifically enhances the heme-dependent growth of the *hem1Δ* yeast strain and is therefore a potential heme transporter. HRG-6::GFP is expressed in the intestine, spermathecal valve and uterus. However, worms expressing the HRG-6::GFP transgene reveal a growth defect at low heme concentrations, which is fully rescued with either the addition of heme or RNAi depletion of *hrg-6*, or *hrg-4*. Surprisingly, CeHRG-6 expression is attenuated by RNAi depletion of *hrg-4*. Our results suggest that CeHRG-6 may function in concert with CeHRG-4 to ensure heme uptake in *C. elegans*, and is plausibly regulated by CeHRG-4 under low heme conditions.

MULTIPLE HRG-1 PARALOGS REGULATE HEME HOMEOSTASIS

IN *C. ELEGANS*

By

Haifa Ben Saidan

Thesis submitted to the Faculty of the Graduate School of the  
University of Maryland, College Park, in partial fulfillment  
of the requirements for the degree of  
Master in Science  
2014

Advisory Committee:  
Professor Iqbal Hamza, Chair  
Professor Caren Chang  
Assistant Professor Antony Jose  
Associate Professor Liqing Yu

© Copyright by  
Haifa Ben Saidan  
[2014]

## **Dedication**

I would like to dedicate this work to my husband, Alsaddeeg Alzarough, and my daughters, Yakeen, Toga, and Baraah. I appreciate all the love and support that you have given me, and the sacrifices that you made during this graduate program. I would also like to dedicate this work to my parents, who were the first to support and foster my love for science.

## **Acknowledgements**

I am grateful to the Molecular and Cell Biology Program for the opportunity to pursue advanced studies in Genetics, and for all of the help and support that they offered along the way. I would like to thank my advisor, Iqbal Hamza and the members of my advisory committee—Caren Chang, Antony Jose, and liqing Yu—who provided assistance for my thesis. Special thanks also go to Xiojing and Tammy, who were always willing to help and proofread this thesis. I received a lot of help from all members of the Hamza lab, through the course of my research. Tamika and Carine were invaluable lab mates, providing advice through my early years in graduate school. To all of Hamza lab members, I say, “thank you.”

I would like to acknowledge the source of funding for my studies, my Libyan government, whose grant has made this research possible. Finally, I would like to thank my family and friends, both here and in Libya; thank you for your continued support and encouragement throughout my graduate studies.

## Table of Contents

Dedication .....	ii
Acknowledgements .....	iii
Table of Contents .....	iv
List of Figures .....	vi
Chapter 1: Literature Review .....	1
Introduction .....	1
Heme biosynthesis .....	2
Transcription regulation by heme .....	9
Heme export .....	10
Heme transporters .....	13
<i>HCPI</i> .....	13
<i>FLVCR2</i> .....	13
<i>HRG-1</i> .....	13
HRG-1 paralogs in <i>C. elegans</i> .....	14
Mild growth delay in double deletion $\Delta$ hrg-1 $\Delta$ hrg-4 mutant worms .....	18
Chapter 2: Materials and methods .....	21
Yeast Assays .....	21
Growth Spot Assay .....	21
Galactosidase Reporter Assay .....	21
Ferric Reductase Assay .....	22
Immunoblotting .....	23
Immunofluorescence .....	23
Statistical Analysis .....	24
Worms assays .....	24
Generation of Reporter Constructs .....	24
Nematode Growth Conditions .....	24
Preparation of Hemin-Chloride .....	25
Worm Synchronization .....	25
RNA-Mediated Interference .....	26
Microparticle Bombardment .....	26
Microscopy .....	27
Worm Growth Assay on RP523 <i>E. coli</i> .....	27
Mammalian Assays .....	28
Cells Transfection for Immunofluorescence .....	28
Fluorescence Protease Protection Assay (FPP) .....	28
Chapter 3: Results .....	30

HRG-6 mediates heme transport in yeast .....	30
Localization of HRG-6 protein in mammalian cells .....	32
Tissue specific expression and subcellular localization of CeHRG-6 in.....	33
<i>C. elegans</i> .....	33
Analysis of genetic interactions between <i>hrg-6</i> and its paralog <i>hrg-4</i> .....	35
 Chapter 4: Discussion .....	 66
 Appendices.....	 71
Appendix I: A cartoon of the FPP illustrates a single cell before and after digitonin and proteinase K treatments.....	71
Appendix II: fluorescence protease protection assay indicates that the C-terminus of HRG-4 is located in the cytosol and the C-terminus of HRG-1 is located within an intracellular compartment. ....	73
Appendix III: The C-terminal domains for both CeHRG-114-CFP and CeHRG-441- CFP are cytoplasmic and are required for proper protein localization. ....	75
Appendix IV: Reporter constructs used in this study. ....	77
Appendix V: Oligonucleotides used in this study.....	78
 Bibliography: .....	 79

## List of Figures

### Chapter 1

Figure 1: heme biosynthesis pathway in eukaryotes.....	3
Figure 2: Schematic model of intracellular heme trafficking. ....	7
Figure 3: Multiple sequence alignment of CeHRG-1, -4, -5 and -6 paralogs has obtained by using ClustalW (v. 1.83). ....	16
Figure 4: Mild growth delay in double deletion $\Delta$ hrg-1 $\Delta$ hrg-4 mutant worms.....	19

### Chapter 3

Figure 1: Improved hemin utilization in yeast overexpressing CeHRG-6 .....	38
Figure 2: Membrane Topology and Localization of CeHRG-4 and CeHRG-6.....	40
Figure 3: Schematic representing hrg-6 transcriptional fusion constructs.....	42
Figure 4: Transgenic worms expressing the Phrg-6(3kb)::HRG-6 SL2::GFP::hrg-6 3'UTR construct express GFP in the intestine.....	44
Figure 5: Localization of HRG-6 in the intestinal cells of <i>C. elegans</i> .....	46
Figure 6: Phrg-6(3Kb)::HRG-6::GFP::hrg-6 3'UTR transgenic worms express HRG-6 on the apical surface of worm's intestine ,uterus, and spermathecal valve of young gravid larval stage. ....	48
Figure 7: Phrg-6(3Kb)::HRG-6::GFP::unc54 3'UTR transgenic worms express HRG- 6 on the apical surface of worm's intestine ,uterus, and spermathecal valve of young gravid larval stage. ....	50
Figure 8: Expression of HRG6::GFP is not regulated by heme. ....	52
Figure 9: Transgenic worms expressing HRG-6::GFP from the 3 kb promoter containing the entire hrg-4 locus show heme-dependent growth arrest. ....	54
Figure 10: Growth arrest of HRG 6::GFP worms at 4 $\mu$ M heme. ....	56
Figure 11: The growth arrest of HRG-6::GFP transgenic worms may be due to hrg-6 overexpression. ....	58
Figure 12: RNAi of hrg-4 at high heme conditions did not have an effect of GFP expression in HRG-6 GFP worm strain.....	60
Figure 13: RNAi of hrg-6 in results in attenuation of HRG-4::GFP expression in the intestine at low heme concentrations. ....	62
Figure 14: Depletion of hrg-4 but not hrg-6 in RNAi-hypersensitive worms results in decreased live progeny when worms are grown at low heme. ....	64

# Chapter 1: Literature Review

## Introduction

Almost all living organisms require iron to maintain life and therefore not surprising iron deficiency anemia is the most common nutritional disorder in the world, and is mainly common in developing countries, where malaria and worm infections are very frequent [1]. According to a World Health Organization report in 2012, 66-80% of the world's population is anemic, mainly due to iron deficiency [2]. A large contribution factor for wide spread iron deficiency anemia is that an estimated four billion people live primarily on plant based diet [3]. Even though plant foods are a good source of iron, they also contain compounds called phytic acids that reduce iron bioavailability [4]. A good bioavailable source of iron, heme-iron, is found in animal protein like red meat [5]. This form is absorbed through the intestine, but little is known about how heme is absorbed and trafficked through intestinal cells.

Heme (iron-protoporphyrin IX) consists of a tetrapyrrole ring with an iron atom residing in the center [6]. Heme is an essential cofactor for many proteins like globins and cytochromes. Heme containing proteins function in diverse biological processes like oxygen transport, xenobiotic detoxification, oxidative metabolism, gas sensing, circadian rhythm, signal transduction, microRNA processing and thyroid hormone synthesis [7-12].

Extensive studies have been done to understand heme synthesis and degradation in eukaryotes. In contrast, heme transport processes remain poorly

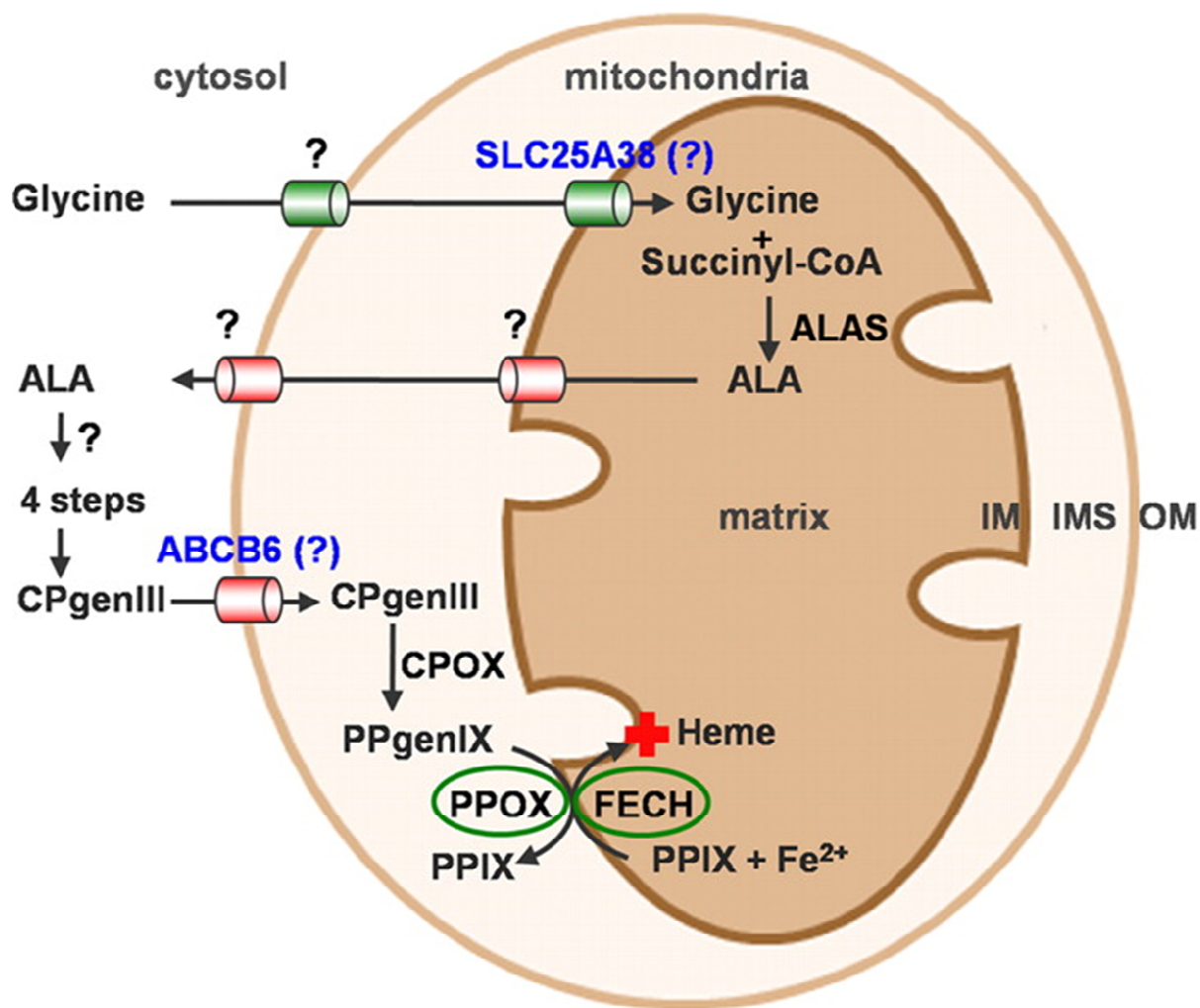
understood because it was difficult to dissociate heme synthesis from trafficking which are normally coordinated. Additionally, mutations in the heme biosynthesis pathways lead to pleiotropic phenotypes and lethality [13]. Our research group has shown that *C. elegans* cannot synthesize heme, but require heme from the environment [14]. Thus, worms are a genetically tractable animal to study the heme transport process without interference from endogenous heme synthesis. Utilizing *C. elegans*, we identified Heme Response Gene-1/4 (HRG-1/4) as the first eukaryotic heme importers. However, the molecular basis for heme transport across biological membranes and whether these heme transporters cooperate with each other to maintain heme homeostasis is unclear. Identification of molecules involved in this pathway will provide novel insights into heme transport processes.

### **Heme biosynthesis**

In most eukaryotes and prokaryotes, heme is synthesized via a highly conserved pathway shared between the mitochondria and the cytosol [15]. In eukaryotes, the first and last three steps occur in the mitochondria, while the other four intermediate steps take place in the cytosol (**Figure 1**). All eight of heme synthesis enzymes are identified and have been studied in detail [16].

**Figure 1: heme biosynthesis pathway in eukaryotes.**

Presumptive heme trafficking pathways that are currently unknown are marked with a (?). In most eukaryotes and prokaryotes, heme is synthesized via a highly conserved pathway shared between the mitochondria and the cytosol. In eukaryotes, the first and last three steps occur in the mitochondria, while the other four intermediate steps take place in the cytosol. The final step of heme synthesis occurs in the mitochondrial matrix. This figure is adapted from [7].



The first step is the condensation of glycine and succinyl-CoA, which results in the formation of 5-aminolevulinic acid (ALA) [17]. This reaction is catalyzed by aminolevulinic acid synthase (ALAS). There are two forms of ALAS [18], where ALAS1 is expressed in all tissue types and ALAS2 is expressed only in erythroid cells. Both ALAS1 and ALAS2 are differentially regulated at the transcriptional level [19]. Mature ALAS is localized to the mitochondrial matrix and requires vitamin B<sub>6</sub> to function correctly [13]. Afterward ALA is transported from the mitochondria to the cytosol by unknown transporter.

After transport to the cytosol, two ALA molecules are condensed by aminolevulinic acid dehydratase (ALAD) to form porphobilinogen (PBG). This reaction is dependent on zinc availability [20]. ALAD is composed of four homodimers with one active site per dimer. Each active site binds to two ALA molecules [21]. One ALA molecule provides the acetate and amino-methyl groups of PBG, while the other ALA molecule is responsible for the propionate side chain and the pyrrole nitrogen [22].

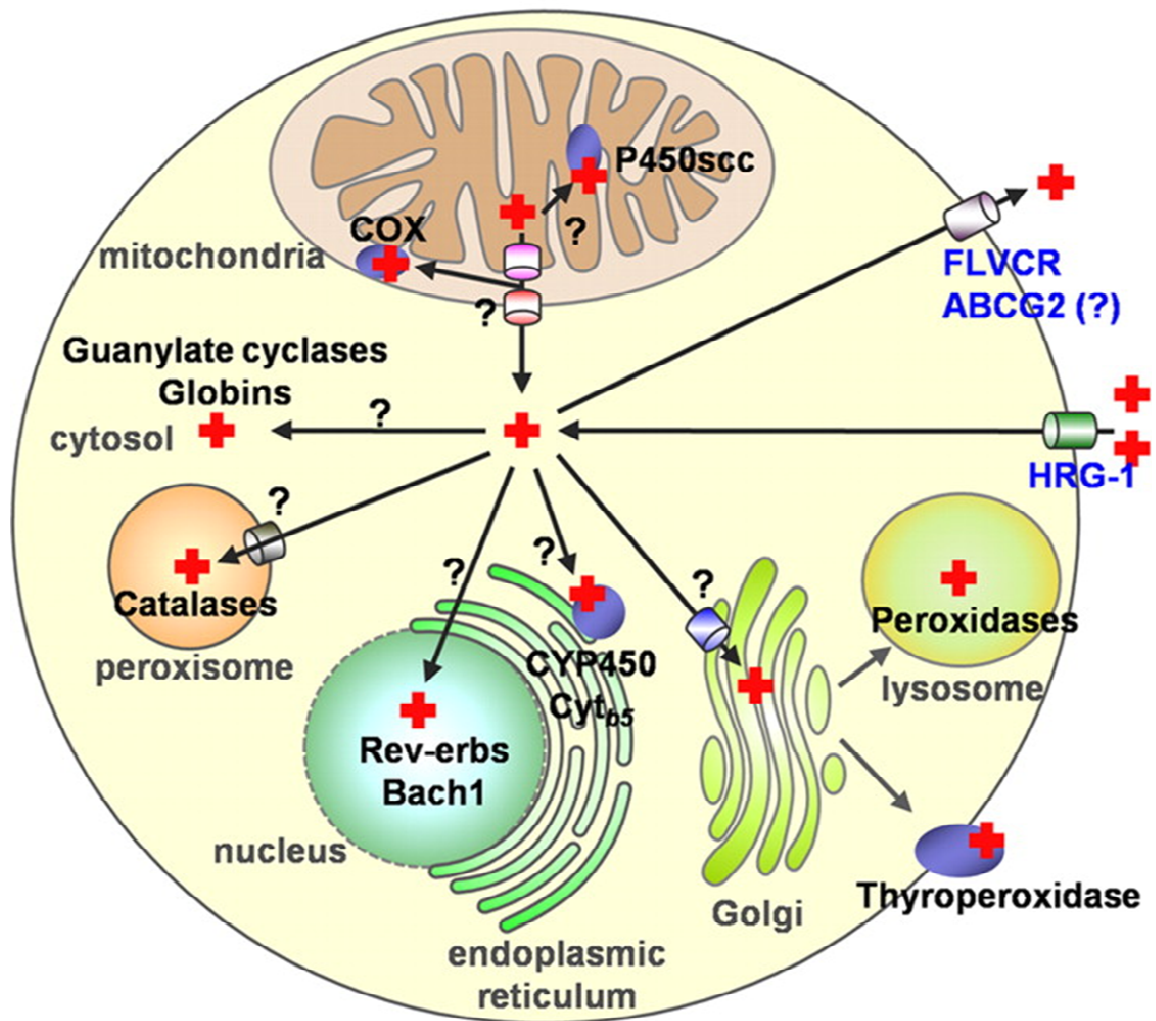
The next two enzymes work to generate a tetrapyrrole. The first reaction is catalyzed by porphobilinogen deaminase (PBGD), which forms the linear tetrapyrrole, hydroxymethylbilane (HMB). Then PBGD binds to HMB and add two additional pyrroles to form hexapyrrole. The four pyrroles distal from the active site of PBGD are cleaved and form HMB [23]. HMB is unstable and must be converted to uroporphyrinogen III (UROgenIII) by uroporphyrinogen III synthase (UROS). UROS catalyzes ring closure to form a tetrapyrrolemacrocycle [13].

The next step is formation of coproporphyrinogen III (CPgenIII) by uroporphyrinogen decarboxylase (UROD). This heme precursor is transported back to the inner mitochondrial space, presumably by ABCB6. However, this finding is still controversial because these studies used the planar oxidized form coproporphyrin III instead of the non-planar reduced CPgen III [24].

The next step is utilization of CPgenIII by coproporphyrinogen oxidase (CPOX), which is localized to the outer mitochondrial membrane with the active site oriented toward the inner mitochondrial space. In this reaction, CPgenIII is converted to protoporphyrinogenIX (PPgenIX) [25]. CPOX is the rate limiting enzyme in heme synthesis pathway [26]. This step is followed by oxidation of PPgenIX to protoporphyrin IX (PPIX) by protoporphyrinogen oxidase (PPOX). This enzyme is localized to the outer surface of the inner mitochondrial membrane and functions as a homodimer [27]. The final step of heme synthesis occurs in the mitochondrial matrix, where iron is inserted into a PPIX ring by ferrochelatase (FECH) to form heme. FECH is located on matrix side of the mitochondrial inner membrane [28]. Heme is somehow exported from the mitochondria to different intracellular compartments, including heme-binding transcription factors in the nucleus, guanylate cyclases and globins in the cytoplasm, cytochromes in the mitochondria, and cyclooxygenases I and II in the endoplasmic reticulum, catalases in peroxisomes, and peroxidases in lysosomes (**Figure 2**) [29].

**Figure 2: Schematic model of intracellular heme trafficking.**

Heme is transported through mitochondrial membranes and incorporated into a multitude of hemoproteins found in different cellular compartments. This process is may be dependent on hemochaperones and transporters. Heme transport proteins that have been already identified are highlighted in blue. Heme can be exported out of the cell or imported into the cell. The cell-surface FLVCR and the ABC transporter ABCG2 have been implicated in heme export in erythroid cells, whereas HRG-1 was identified as a heme importer. Question marks represent the presumptive heme trafficking pathways. This figure is adapted from [7].



## Transcription regulation by heme

Heme has been shown to be involved in transcription regulation of many genes that function in circadian rhythm and oxidative respiration. According to microarray data from K562 cells, there are several genes transcriptionally regulated by heme [7]. It has been shown that the levels of Bach1, an endogenous basic leucine zipper protein (bZip), were significantly decreased in the presence of heme [30]. By contrast, treatment with succinylacetone, the inhibitor of heme biosynthesis, resulted in higher Bach1 levels in murine embryonic fibroblasts. Another heme-regulated gene that is involved in circadian clock control is the nuclear hormone receptor Rev-Erba [11].

Heme has a role in transcriptional regulation of hemoglobin production. Under low heme conditions, globin chain production is reduced. Bach1 regulates the transcription of globin by binding to MARE sequences (Maf Recognition Element), which is located 60 kb upstream of globin genes. This leads to recruitment of Maf proteins which activate or repress globin genes expression according to heme conditions [31].

In order to identify genes that are regulated by heme, our group performed affymetrix whole genome microarray on *C. elegans* grown at low (4  $\mu$ M), optimal (20  $\mu$ M), and high (500  $\mu$ M) heme levels. The results showed that 288 genes have altered expression levels at high or low heme when compared to optimal heme conditions. These genes are classified as heme-responsive genes (*hrgs*). Among these genes, there are 41 transmembrane proteins predicted by TMHMM 2.0 [13, 32].

## Heme export

Living cells export heme to prevent heme toxicity and cellular damage. FLVCR1 and ATP-binding cassette transporter G2 (ABCG2) have been identified as heme exporters in humans. FLVCR was identified as a cell surface receptor for feline leukemia virus subgroup c receptor [33]. FLVCR1 shows tissue specific expression in hematopoietic cells and is weakly expressed in the fetal liver, kidney and pancreas [34]. FLVCR1 has been shown to reduce intracellular heme levels and mediate efflux of the fluorescent heme analog, zinc mesoporphyrin (ZnMP), in hematopoietic K562 cells [35]. Knock out of FLVCR1 in mice results in failure of erythroid differentiation and death at midgestation stage [36]. These mice also have limb deformities and cranio-facial defects that are similar to the symptoms of patients with rare congenital erythroid anemia and Diamond-Blackfan anemia (DBA). The current model postulates that FLVCR1 exports heme when macrophages phagocytose senescent red blood cells (RBCs) [36].

Interestingly, Tolosano *et al* recently showed that there is another FLVCR1 isoform, FLVCR1b, which is a smaller protein that localizes to the mitochondria. Knockdown of *FLVCR1b* results in mitochondria heme accumulation, indicating that FLVCR1b is a mitochondrial heme exporter. In contrast, targeted deletion of *FLVCR1a* resulted in skeletal defects and vascular abnormalities. Recently, four missense mutations in FLVCR1 have been found in patients with the rare autosomal recessive disease posterior column ataxia and retinitis pigmentosa (PCARP) [37, 38]. Three of the four mutations occur in exon 1 of the gene and are FLVCR1a specific.

However, none of the patients carrying these gene variations is anemic. The physiological role of FLVCR1 remains unknown [38].

ABCG2 was initially discovered as breast cancer resistance protein (BCRP) that causes drug resistance in breast cancer cells and identified as a second heme exporter in mammals [39]. *ABCG2* knockout mice that were fed modified diet showed skin photosensitivity [40]. The reason behind photosensitivity is accumulation of pheophorbide A, which is a degradation product of chlorophyll and is similar to PPIX [41].

Our research group performed genome-wide analysis and identified MRP-5 as an intestinal heme exporter in *C. elegans* [42]. This inference is based on the fact that *mrp-5* is upregulated in response to heme deficiency [43], depletion of *mrp-5* by RNAi results in embryonic lethality which can be rescued by growth in the presence of excess heme, and that RNAi depletion of *mrp-5* results in accumulation of ZnMP in worm intestinal cells. MRP-5 is the homolog of human ABC transporter ABCC5, which could possibly be a heme exporter in humans.

Senescent red blood cells are phagocytosed by macrophages of the reticuloendothelial system, where their contents are digested and recycled. Heme released from engulfed RBCs is degraded by heme oxygenase-1 (HO-1) in macrophages. Heme is broken down to biliverdin, carbon monoxide and iron. Then biliverdin is converted to bilirubin by biliverdin reductase. Iron is either stored in ferritin or exported out of macrophages by the iron exporter, ferroportin-1 (FPN1, SLC40A1) [44].

Iron in the circulation is found associated with a protein called transferrin. When a cell requires iron, transferrin receptors are directed to plasma membrane to absorb iron-transferrin complexes by receptor-mediated endocytosis. Once internalized in coated vesicles, the complexes get delivered to early endosomes, where the acidic pH results in the release of  $\text{Fe}^{3+}$  from the protein. Iron is reduced in the endosomal compartments and then exits to the cytoplasm. The transferrin receptor and its cargo of transferrin are recycled to the plasma membrane, where the transferrin detaches from the receptor to re-enter the circulation [44, 45].

## **Heme transporters**

### *HCP1*

Heme carrier protein 1 (HCP1/SLC46A1) is a membrane protein expressed by enterocytes in the duodenum [46]. Over expression of *HCP1* in *Xenopus* oocytes resulted in increased heme uptake; however, other studies have shown that folate transport by this protein is higher than that observed with heme, suggesting that folate might be the physiological ligand for HCP1. *HCP1* knockout mice showed macrocytic normochromic anemia, which could be fully rescued with folate supplementation, indicating defective folate transport, rather than a defect specific to heme or iron. RNA interference assays of *HCP1* in CaCo-2 cells resulted in reduction heme and folate uptake but increase HO-1 expression [47].

### *FLVCR2*

Feline leukemia virus subgroup C receptor 2 (FLVCR2) was recently reported to import heme in mammalian cells [48]. Depletion of *FLVCR2* by RNAi in human cells significantly decrease uptake of the fluorescent heme analog. However, ectopic expression of FLVCR2 does not rescue growth of a heme-deficient yeast strain. It is possible that FLVCR2 may efflux heme because it is a homolog of the heme effluxer FLVCR [32, 34, 49]. Currently, the physiological role of FLVCR2 is still unclear.

### *HRG-1*

HRG-1 is located in endo-lysosomal compartments within intestinal cells in worms, releasing stored heme into the cytoplasm under low heme conditions [43]. Transient knockdown of *hrg-1* in zebrafish results in hydrocephalus, yolk tube

malformations and severe anemia. CeHRG-1 fully rescued all phenotypes observed due to knockdown of *hrg-1* in zebrafish. Additionally, significant heme-induced inward currents were observed in *Xenopus* oocytes injected with cRNA for HRG-1, indicating heme-dependent transport across cell membranes [43]. We and others have recently found that *hrg-1* localized to the lysosomal compartments in HEK293 cells [43], and is also recruited and localizes to the erythrophagosomal membrane in bone marrow derived macrophages (BMDMs) after ingesting RBCs [50].

### **HRG-1 paralogs in *C. elegans***

To elucidate the role of these genes in heme homeostasis, we established RNAi assays in worms grown at various heme concentrations. The heme sensor IQ6011 strain (*Phrg-1::gfp*) expresses GFP specifically in the intestinal cells of larvae and adult worms. GFP is upregulated at low heme and downregulated at high heme. Depletion of *hrg-4* in this strain resulted in increased GFP expression [43]. Knockdown of *hrg-4* in wild type worms resulted in resistance to the cytotoxic heme analog, gallium protoporphyrin IX (GaPP). Depletion of *hrg-4* in wild type worms by RNAi resulted in no detectable ZnMP uptake in the intestine. A fusion of HRG-4 protein to GFP localizes to the apical intestinal membrane. Taken together, these results indicate that HRG-4 functions as an intestinal heme importer at low heme in *C. elegans*.

BLAST analysis of the *C. elegans* genome showed that *hrg-1* and *hrg-4* had two other paralogs, *hrg-5* and *hrg-6*. *hrg-6* is separated from *hrg-4* by 1.6kb and they are divergent in the orientation of the ORF on chromosome IV. *hrg-4*, *hrg-5* and

*hrg-6* are nematode-specific genes, whereas *hrg-1* has orthologs with about 21% amino acid identity in vertebrates. Whereas the expression of *hrg-1* and *hrg-4* are highly regulated by heme, *hrg-5* and *hrg-6* are not heme responsive. A multiple sequence alignment of HRG-1, -4, -5 and -6 paralogs was obtained using ClustalW (v. 1.83) [31] as shown in **(Figure 3)**. We identified highly conserved residues that are important for CeHRG-1 and CeHRG-4 mediated heme transport, including invariant histidine/tyrosine in TMD2, a specific histidine in the 2nd exoplasmic loop E2 and the FARKY motif [51].

**Figure 3: Multiple sequence alignment of CeHRG-1, -4, -5 and -6 paralogs has obtained by using ClustalW (v. 1.83).**

Identical amino acids and conservative changes are indicated by reversed and shaded characters, respectively. Asterisk indicates conserved histidines in CeHRG-1 that are replaced by tyrosines in CeHRG-4 and CeHRG-6. Boxed residues denote the four putative transmembrane domains based on predictions by TMHMM 2.0 and SOSUI [31]. Amino acids shaded red is potential heme binding residues. HRG-1 proteins share certain characteristics with tetraspanin proteins, including polar residues (gray), and cysteines within TMDs that serve as putative palmitoylation sites. This figure is adapted from [43].

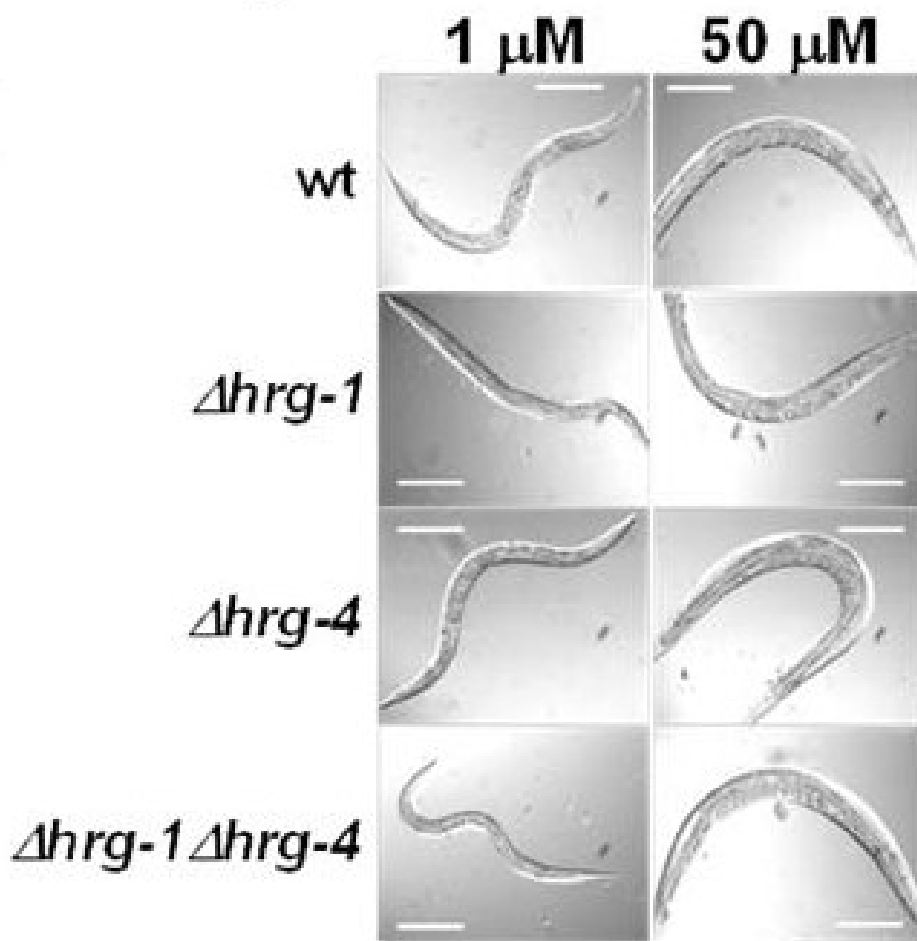


### **Mild growth delay in double deletion *Δhrg-1Δhrg-4* mutant worms**

The *Δhrg-1Δhrg-4* mutant worms were growth delayed only at low heme corresponding to a delay of up to three larval stages during development. They were synchronized and placed on 50 μM heme NGM plate (P0) then synchronized again and transferred (F1) to both low and high heme NGM plates. Growth defect was observed after two subsequent generations (**Figure 4**). Most importantly, the growth delay was fully rescued when the mutant worms were fed a heme-rich diet [51]. This phenotype observed in the *Δhrg-1Δhrg-4* mutants indicate worms have other ways to acquire heme, possibly via HRG-1 paralogs which may provide the compensatory mechanisms for heme uptake in the worms that lack *hrg-1* and *hrg-4*. The present study was conducted to identify if HRG-1 paralogs cooperate with each other to maintain heme homeostasis.

**Figure 4: Mild growth delay in double deletion *Δhrg-1Δhrg-4* mutant worms.**

Wild-type, *Δhrg-1*, *Δhrg-4* and *Δhrg-1Δhrg-4* worms were synchronized, placed on NGM plates seeded with RP523 bacteria grown at 50 μM heme (P0), synchronized again and transferred to RP523 plates of low (1 μM) and high (50 μM) heme (F1) and follow the growth for two subsequent generations (F2). The images represent F2 progeny. “This figure is adapted from” [51].



## Chapter 2: Materials and methods

### Yeast Assays

#### Growth Spot Assay

Plasmids encoding HRG-1 transporters were transformed into the yeast *hem1Δ* strain using lithium acetate method [52]. Transformants were selected on 2% w/v glucose SC (-Ura) plates supplemented with 250 μM ALA. Five or six transformed colonies were picked and streaked on 2% w/v raffinose SC (-Ura) plates supplemented with 250 μM ALA to deplete glucose for 48 hours. Before splitting, cells were cultivated in 2% w/v raffinose SC (-Ura) medium for 18 hours to deplete heme. Cells were then diluted to an OD600 of 0.2. Ten-fold serial dilutions of each transformant were spotted (10 μL /spot) onto 2% w/v raffinose SC (-Ura) plates supplemented with either 0.4% w/v glucose and 250 μM ALA (positive control), or 0.4% w/v galactose and different concentrations of hemin, and incubated at 30°C for 3 days before imaging [51].

#### Galactosidase Reporter Assay

Plasmids encoding vector, CeHRG-4 and CeHRG-6 were co-transformed into the yeast *hem1Δ* strain together with the pRS314m-CYC1-LacZ plasmid. Selection of transformants was performed as described above using SC auxotrophic medium supplemented with 250 μM ALA. Cells were depleted for hemin in 2% w/v raffinose SC (-Ura, -Trp) medium for 12 hours, and then were suspended at an OD600 of 0.1 in

10 mL 2% w/v raffinose SC (-Ura, -Trp) medium supplemented with 0.4% w/v galactose, and different concentrations of hemin. Cells were cultivated at 30°C, with shaking at 225 rpm for 12 hours [51], and assayed for galactosidase activity, as described elsewhere[53]. Galactosidase activities were normalized to total protein concentration for comparison.

### **Ferric Reductase Assay**

Plasmids encoding vector, CeHRG-4 and CeHRG-6 were transformed into the *hem1Δ- fre1Δ- fre2ΔMET3-FRE1*. Cells were depleted for heme in 2% w/v raffinose SC (-Ura, -Trp-Met) medium for 12 hours, and then were suspended at OD600 of 0.3 in 2% w/v raffinose SC (-Ura, -Trp-Met) medium supplemented with 0.4% w/v galactose, 0.1 mM Na<sub>2</sub>S, and different concentrations of hemin. Cells were then cultivated in 96-well plates at 30°C, with shaking at 225 rpm for 16 hours [51], and assayed for ferric reductase activity [54]. Cells were washed with washing buffer (2% BSA, 0.1% tween-20 in 2× PBS) three times to remove hemin in the medium, then washed twice with reaction buffer (5% glucose, 0.05 M sodium citratebuffer, pH 6.5). They were suspended in reaction buffer and their OD600 was measured using a platereader (BioTek). The assay buffer (2mM bathophenanthrolinedisulfonate (BPS), 2mM FeCl<sub>3</sub> in reaction buffer) was added to the cells. The cells were incubated in the dark at 30°C until red color was developed. OD535 and OD610 of the incubated cells were measured and ferric reductase activity (nmol/10<sup>6</sup> cells/min) was calculated [51].

### **Immunoblotting**

For Western blotting experiments, yeast transformants were resuspended in lysis buffer (1% SDS, 8 M urea, 10 mM Tris-HCl pH 8.0, 10 mM EDTA) with protease inhibitors (1 mM phenylmethylsulfonyl fluoride, 4 mM benzamide, 2 µg/mL leupeptin, and 1 µg/mL pepstatin) and 0.5 mm acid-washed glass beads. Cells were heated at 65°C for 10 min and broken using FastPrep-24 (MP Bio) for 3×30s at the 6.5m/s setting. The total protein concentration was quantified with the Bradford reagent (Bio-Rad). Protein samples were separated on 12% SDS-polyacrylamide gel and transferred to nitrocellulose membrane (Bio-Rad). The membranes were incubated with rabbit anti-HA (Sigma) as primary antibody at a 1:1,000 dilution overnight at 4°C, followed by HRP-conjugated goat anti-rabbit antibody at a 1:10,000 dilution for 1 hour at room temperature. Signal was detected using Super Signal chemiluminescence reagents (Thermo Scientific) in the Gel Documentation system (Bio-Rad) [51].

### **Immunofluorescence**

Yeast transformants were cultivated in 2% w/v raffinose SC (-Ura) medium supplemented with 0.4% w/v galactose and 250 µM ALA for 12 hours and then fixed with 4% formaldehyde for 1 hour at room temperature. Immunofluorescence microscopy was performed as described elsewhere [53]. Images were taken using a DM IRE2 epifluorescence microscope (Leica) connected to a Retiga 1300 cooled mono 12-bit camera.

## Statistical Analysis

Statistical significance was calculated by using one-way ANOVA with the Student–Newman–Keuls multiple comparison test in GraphPad INSTAT version 3.01 (GraphPad, San Diego). Data values were presented as mean  $\pm$  SEM. A p value  $< 0.05$  was considered significant.

## Worms assays

### Generation of Reporter Constructs

*Phrg-6::hrg-6::ICS::GFP::hrg-6 3'-UTR*, *Phrg-6(1.6kb)::hrg-6::GFP::hrg-6 3'-UTR*, *Phrg-6(3kb)::hrg-6::GFP::hrg-6 3'-UTR* *Phrg-6(3kb)::hrg-6::GFP::hrg-6 unc45 3'-UTR*, *vha-6::hrg-6::GFP::hrg-6 3'-UTR*, *Phrg-6::hrg-6::GFP::hrg-6 3'-UTR*, *Phrg-6::hrg-6 FLAG::ICS::GFP::hrg-6 3'-UTR* and *Phrg-4::hrg-4 FLAG::ICS::GFP::hrg-4 3'-UTR* plasmids were constructed using the Gateway cloning system (Invitrogen). The promoter of interest, the *gfp* gene, and the 3'UTR belonging to the gene or of the generic *unc-54* 3'UTR were cloned by recombination into the entry vectors pDONR-P4-P1R, pDONR-221, and pDONRP2R-P3, respectively, using the Gateway BP Clonase kit. The three entry clones were then recombined into a single destination vector, pDEST-R4-R3, using the Gateway LR Clonase II Plus enzyme kit.

### Nematode Growth Conditions

*C. elegans* strains were maintained on nematode growth medium (NGM) agar plates seeded with OP50 bacteria at 20°C. For genotyping, individual worms were lysed in

5  $\mu$ l lysis buffer (50 mM KCl, 10 mM Tris-HCl, 2.5 mM MgCl<sub>2</sub>, 0.45% NP-40, 0.45% Tween-20, 0.01% gelatin, and 1mg/ml freshly prepared proteinase K) by freezing and heating (2 hours at -80°C, 1 hour at 65°C, and 30 min at 95°C). Worm lysates were then subjected to PCR reactions.

### **Preparation of Hemin-Chloride**

130 mg of hemin chloride (Frontier CAS#16009-13-8) was added to 18 ml of 0.3 M NH<sub>4</sub>OH. Concentrated HCl was added until the solution had a pH of 7.5-8.0. The solution was brought to 20 ml with 0.3 M NH<sub>4</sub>OH, pH 8.0, to give a final concentration of 10 mM hemin chloride.

### **Worm Synchronization**

Nematodes were centrifuged at 800 x g for 5 minutes. The worms were then suspended in 10 ml of 0.1 M NaCl and allowed to settle on ice for 5 min. After that, the supernatant was aspirated and 6 ml of 0.1 M NaCl was added to the worm pellet. 1 ml of 5M NaOH was mixed with 2 ml of 5% bleach in a separate tube. The NaOH /bleach solution was mixed with the nematode population. The suspension was intermittently vortexed for 5 min until the cuticles of gravid worms dissolved and the eggs were released, then immediately worms were centrifuged at 800 x g for 45 sec. The supernatant was aspirated, and 10 ml sterile water was added to the egg pellet and vortexed for 5 sec. The suspension was centrifuged at 800 x g for 45 sec. After that, adding water and centrifugation step was repeated to wash the bleach solution. The worms pellet was resuspended in 10 ml M9 salt solution (86 mM NaCl, 42 mM

Na<sub>2</sub>HPO<sub>4</sub>, 22 mM KH<sub>2</sub>PO<sub>4</sub>, 1 mM MgSO<sub>4</sub> 7H<sub>2</sub>O). The eggs incubated overnight in the M9 solution at 20°C on a platform shaker to 70 rpm.

### **RNA-Mediated Interference**

The transgenic worms were initially maintained on nematode growth medium (NGM) agar plates seeded with OP50 bacteria at 20°C. Synchronized L1 larvae were then exposed to HT115 (DE3) *E. coli* expressing *vector*, *gfp*, *hrg-1*, *hrg-4*, or *hrg-6* double stranded RNA from the Ahringer Library were grown in LB broth supplemented heme for 5.5 h [55]. Two wells of a 12-well nematode growth medium-agar plate were spotted with bacteria transformed with each construct and allowed to induce for 24 h with 1 mM isopropyl -D-thiogalactopyranoside. GFP expression in the worms was analyzed 72 h after RNAi feeding with a Leica MZ16 FA stereomicroscope. Images were acquired with a Leica DMIRE2 inverted microscope equipped with a CCD camera.

### **Microparticle Bombardment**

Mutant *unc-119* (*ed3*) worms were grown for 7 days in flasks containing 90 ml meCHR-2 media supplemented with 20 µM heme. The worms were then transferred to 50 ml conical tubes and allowed to settle. The supernatant was aspirated to remove larvae, which take longer time to settle than gravid worms. The gravid worms were spread evenly onto 10 cm<sup>2</sup> NGM agar plate and incubated on ice for 30 min. After the incubation, *unc-119* (*ed3*) gravid hermaphrodite animals were co-bombarded with 10 µg of reporter construct and 5 µg of the *unc-119* rescue plasmid (pDM016B) using

the PDS-1000 particle delivery system (Bio-Rad) which was carried out following the protocol described by Praitis et al. [56]. The DNA mixture was coated onto 2 $\mu$ M gold beads. The worms were washed from bombardment plates and transferred to plates seeded with a lawn of *E. coli* JM109. After 2 weeks incubation at 25 °C, wild-type F2 worms were removed from plates and maintained as transformed strains.

### **Microscopy**

GFP levels were analyzed by fluorescence microscopy with a Leica MZ16 FA stereomicroscope. The worms were immobilized in 10 mM levamisole on a 2% agarose pad affixed to a slide. Differential interference contrast (DIC) and fluorescence images were taken with a Leica DMIRE2 inverted microscope attached to a CCD Retiga 1300 camera controlled by Simple PCI software (Hamamatsu, Bridgewater, NJ).

### **Worm Growth Assay on RP523 *E. coli***

The heme-deficient *E. coli* strain RP523 [57] was grown overnight in Luria-Bertani medium supplemented with 1  $\mu$ M heme. The bacteria were diluted at a ratio of 1:6 into fresh LB medium supplemented with different concentrations of hemin and cultivated for 5.5 hours. The OD600 of these bacteria was determined and the culture was diluted to OD600 = 0.5 with corresponding LB medium. Each 35 mm NGM plate was seeded with 200  $\mu$ l cell culture. Synchronized L1 larvae grown on OP50-seeded NGM plates were transferred onto NGM plates seeded with RP523

grown with 4, 20, and 50  $\mu$ M hemin, and incubated at 20°C for 4 days (P0). The worms were imaged using a DMIRE2 epifluorescence microscope (Leica).

## **Mammalian Assays**

### **Cells Transfection for Immunofluorescence**

HEK293 cells were maintained in Dulbecco's modified medium with 10% fetal bovine serum, 1% penicillin-streptomycin, and glutamine. HEK293 cells were seeded on glass coverslips and transfected with FuGENE 6 the following day at a confluence of 50%. FuGENE 6 transfection was performed according to the manufacturer's protocol, and cells were fixed two days after transfection and then analyzed by microscopy.

### **Fluorescence Protease Protection Assay (FPP)**

The FPP Assay was carried out as previously described [58]. HEK293 cells were grown in LabTeK cover glass culture chambers (Nunc) and transfected with pECFP-N1 HRG-1 chimera constructs. Cultures were incubated for 24 hours and then the cells were washed three times with KHM buffer (20 mM HEPES, pH 6.5, 110 mM potassium acetate, and 2 mM  $MgCl_2$ ). Images of selected cells were recorded using a DMIRE2 epifluorescence microscope (Leica) connected to a Retiga 1300 cooled Mono 12-bit camera. Time-lapse images were acquired before and after proteinase K (50 mg/ml for 3 minutes) digestion. Following this, the cells were

treated with both 30 mM digitonin and proteinase K and images were recorded 1, 2 and 3 minutes after treatment.

## Chapter 3: Results

### HRG-6 mediates heme transport in yeast

Our genetic investigations of *C. elegans* clearly indicate that CeHRG-1 and CeHRG-4 function to maintain heme homeostasis in worms. The presence of multiple paralogs of HRG-1 proteins in *C. elegans* makes it difficult to assess the function of each HRG-1-paralog individually. In order to assess CeHRG-6 for heme transport activity, we used yeast assays that have been extensively utilized in our lab [59]. We used *Saccharomyces cerevisiae hem1Δ* mutants that cannot make heme because they lack  $\delta$ -aminolevulinic acid synthase (ALAS), which is required for synthesis of  $\delta$ -aminolevulinic acid (ALA), a precursor for heme synthesis. The *hem1Δ* mutant yeast strain is unable to grow in the presence of low amounts of heme because it utilizes exogenous heme poorly. This growth defect can be rescued by supplementation with increasing concentrations of exogenous heme or the heme precursor ALA [60]. The growth of this yeast in the presence of low heme (0.05  $\mu$ M) can also be rescued with the ectopic expression of heme importers like CeHRG-1 or CeHRG-4 [51].

HRG-1-related proteins tagged at the C-terminus with a HA epitope were expressed in *hem1Δ* using the yeast-specific expression vector, pYES-DEST52, under control of the GAL1 promoter, which is induced in the presence of galactose and repressed by adding glucose. The degree of growth rescue and the heme concentration indicate relative uptake of heme by HRG-1 related proteins. For proper interpretation of the results from the yeast reporter assays, first we determined the subcellular localization of ectopically expressed CeHRG-6 in yeast. CeHRG-6-HA

was inserted into the yeast expression plasmid and transformed into *hem1Δ* yeast. Expression of CeHRG-6-HA was probed using an anti-HA antibody and it was localized using immunofluorescence and confocal microscopy. The data confirmed that CeHRG-6-HA was localized to the plasma membrane of yeast in a manner similar to CeHRG-4-HA (**Figure 1A**). Western blot analysis performed on yeast expressing CeHRG-4-HA and CeHRG-6-HA showed that both proteins were expressed at equal levels (**Figure 1B**). Similar to the expression of the heme importers, CeHRG-4-HA, CeHRG-1-HA, and human HRG1-HA, expression of CeHRG-6-HA resulted in increasing yeast growth in the presence of low heme when compared to cells transformed with empty vector (**Figure 1C**). Data showed that both CeHRG-4-HA and HRG-6-HA rescue the yeast growth better than CeHRG-1-HA and human HRG-1-HA.

In order to determine if expression of CeHRG-6 resulted in a change in cytoplasmic heme levels, we took advantage of the yeast transcription factor, Hap1p, which activates the *CYCI* promoter in the presence of heme. Under low heme conditions, Hap1p is localized in the nucleus but remains inactive in large protein complexes. When heme is available, Hap1p dissociates from these complexes and activates *CYCI*, which encodes iso-1- cytochrome c, required for aerobic respiration [61]. To monitor heme availability in the cytosol, we used a *CYC1::lacZ* promoter reporter fusion. Expression of either CeHRG-4-HA or CeHRG-6-HA resulted in increased  $\beta$ -galactosidase activity significantly further confirming both CeHRG-4 and CeHRG-6 are capable of transporting heme into the cytosol (**Figure 1D**).

To measure heme availability in an intracellular compartment, we used a *hem1Δfre1Δfre2ΔMET3-FRE1* yeast strain engineered to constitutively express a single ferric reductase from the PGK1 promoter [59]. Ferric reductases are heme-dependent plasma membrane proteins that function to reduce iron from Fe<sup>3+</sup> to Fe<sup>2+</sup> before it can be imported into the cell. Ferric reductases receive their heme within the secretory pathway, and thus ferric reductase activity can be used as a measurement of heme availability in the secretory pathway. Similar to CeHRG1-HA and CeHRG4-HA, expression of CeHRG6-HA in this system resulted in increased ferric reductase activity significantly in the presence of low heme (**Figure 1E**). Our interpretation of these data is that CeHRG-6 is importing heme into the yeast cell which becomes available to the secretory pathway through an as yet unknown mechanism. Together, these studies strongly demonstrate that HRG-1 related proteins transport heme in yeast as a heterologous system. Although these yeast experiments were strongly suggestive that CeHRG-6 can import heme, we conducted additional experiments in *C. elegans* and mammalian cells to confirm the membrane localization and heme transport activity of CeHRG-6.

### **Localization of HRG-6 protein in mammalian cells**

We next wanted to determine whether CeHRG-6 shared topological and localization features with CeHRG-4 given the growth pattern and membrane localization of these two proteins in yeast (**Figure 2A**). Our studies have previously found that most worm proteins localize to similar membrane compartments when expressed in mammalian cells. For example, CeHRG-4 is found on the plasma membrane of worm's intestinal cells and when expressed in non-polarized HEK293

cells (**Figure 2B**). Our results reveal that YFP tagged CeHRG-6 also localizes to the plasma membrane in HEK293 cells, in support of the cell surface localization seen for CeHRG-6 expressed in worm intestinal cells (**Figure 2A**). Indeed FPP assays using CeHRG-1 and CeHRG-4 or chimeras in HEK293 cells indicate that the C-terminus of both proteins is cytoplasmic (**Appendices I & II& III**).

### **Tissue specific expression and subcellular localization of CeHRG-6 in**

#### ***C. elegans***

To determine which tissues express *hrg-6* and evaluate the regulation of its expression, *hrg-6 promoter::GFP::hrg-6* 3'UTR constructs were generated using the MultiSite Gateway system (Invitrogen) and transformed into worms by microparticle bombardment. *hrg-4* and *hrg-6* are found in tandem on chromosome IV, where they are separated by 1.6 kb and divergent in gene orientation. Two different promoters were used: a 1.6 kb upstream sequence of *hrg-6* which included the intergenic region between *hrg-4* and *hrg-6* (**Figure 3A**), and a 3 kb sequence upstream of *hrg-6* which also included *hrg-4* and its 3'-UTR (**Figure 3B**). None of these constructs expressed detectable GFP signals in the transgenic worms. A third construct was generated which contained the 3 kb promoter and included *hrg-6* separated from *gfp* by an SL2 intercistronic sequence (ICS): *Phrg-6::hrg-6::ICS::GFP::hrg-6* 3'-UTR (**Figure 3C**). The SL2 sequence engineered between two genes results in both genes being transcribed into a single RNA, which is then spliced and subsequently translated into two separate proteins [62]. The advantage of this construct is that there is no interference from the GFP tag to the protein of interest, but expression of GFP is

indicative of transgene expression. Interestingly, this transgenic worm strain expressed GFP in the intestine, indicating that intergenic regions within *hrg-6* are required for *hrg-6* expression (**Figure 4**).

To examine the subcellular localization of CeHRG-6 protein, translational reporter constructs containing the 1.6 kb and 3 kb upstream sequences as described above were generated. This was done using a PCR reaction to fuse HRG-6 to GFP, which was cloned into the entry vector pDONR-221 using the MultiSite Gateway system (Invitrogen). Both of the upstream sequences of *hrg-6* promoter and the *hrg-6* 3'UTR were cloned by recombination into entry vectors pDONR-P4-P1R, and pDONR-P2R-P3, respectively, using the Gateway BP Clonase kit. The three entry clones were then recombined into a single destination vector, pDEST-R4-R3, using the Gateway LR Clonase II Plus enzyme kit. The final construct is the HRG-6 ORF fused to GFP, downstream of the putative *hrg-6* promoter and upstream of the *hrg-6* 3' untranslated region. This construct was then transformed into the worm by microparticle bombardment. The subcellular localization of HRG-6 in transgenic worms was determined using fluorescence microscopy and confocal imaging. Both HRG-6::GFP expression from the 1.6 kb upstream promoter and from the intestinal-specific *vha-6* promoter is mainly on the apical surface of intestine (**Figure 5A&B**). However; the 3 Kb upstream construct, *Phrg-6(3Kb)::HRG-6::GFP::hrg-6* 3'UTR worms, expressed HRG-6 on the apical plasma membrane of the whole intestine at all larval stages, uterus of young adult stage and spermathecal valve of young gravid larval stage (**Figure 6**). Changing the 3'UTR of this transgene to the generic *unc-54* 3'UTR did not change the expression pattern of CeHRG-6 (**Figure 7**). These data

indicate that the functional 3 Kb *hrg-6* promoter includes the entire *hrg-4* gene and that HRG-6 is expressed in all intestinal cells, uterus and spermathecal valve.

#### **Analysis of genetic interactions between *hrg-6* and its paralog *hrg-4***

We sought to determine the effect of varying heme concentrations on the CeHRG-6 translational reporter worm stains. *Phrg-6(3Kb)::HRG-6::GFP::hrg-6* 3'UTR reporter worms were fed the heme-deficient *E.coli* strain, RP523, grown at 4, 20, and 50  $\mu$ M heme [57]. This bacterial strain requires exogenous heme for growth, which permits greater control of heme concentrations supplied to the worm than regular OP50 bacteria. In contrast to HRG-4::YFP transgenic worms in which YFP fluorescence was repressed at high heme concentration, HRG-6::GFP transgenic worms showed no change in GFP expression at different heme concentrations (**Figure 8**). This is consistent with our microarray studies, indicating that CeHRG-6 expression is not regulated by heme levels in worms even at 500  $\mu$ M heme [43]. It is also suggestive of the notion that CeHRG-6 functional across a wider range of heme concentrations compared to CeHRG-1 and CeHRG-4, which are not expressed beyond 20  $\mu$ M heme.

Surprisingly, transgenic worms expressing HRG-6::GFP from the 3 kb upstream sequence containing the entire *hrg-4* locus showed growth arrest at low heme conditions and this phenotype could be rescued by addition of heme (**Figure 9**). Changing the 3'UTR of this transgene to the generic *unc-54* 3'UTR did not rescue this growth defect, indicating that HRG-6 3'UTR has no effect on the growth arrest phenotype. Both HRG-6::GFP expressed from the 1.6 kb upstream promoter and from the intestinal-specific *vha-6* promoter did not show a growth arrest but revealed

a slight growth delay comparing to wild type worms (**Figure 10**). These results are suggestive that either *hrg-6* expression is not as strong in these constructs as from 3 kb upstream sequence or that overexpression of HRG-6 has a negative effect on HRG-4, which is present in the 3 kb promoter, under low heme conditions.

RNAi depletion is a good genetic tool to study the interaction between *hrg-6* and *hrg-4* and to confirm that the growth arrest for CeHRG-6 reporter worms is due to CeHRG-6 overexpression. RNAi of *gfp* or *hrg-6* in *Phrg-6(3kb)::HRG-6::GFP::hrg-6* 3'UTR transgenic worms rescued the growth arrest phenotype (**Figure 11A**). By contrast, knockdown of either *vector* or *hrg-1* did not rescue the growth arrest phenotype. These results indicate that the growth arrest is possibly because of *hrg-6* overexpression. RNAi of *hrg-4* at low heme concentrations in this transgenic worm strain resulted both in the attenuation of HRG-6::GFP expression only in the intestine and not in spermathecal-uterine valve as well as rescue of the growth arrest phenotype (**Figure 11A**). Also, RNAi of *hrg-4* resulted in depletion of *hrg-6::ICS::GFP* (**Figure 11B**). RNAi of *hrg-4* at high heme conditions did not have any effect of GFP expression in this worm strain (**Figure 12**). These results suggest that CeHRG-4 and CeHRG-6 interact at a post-transcriptional level.

To further investigate the genetic interaction between *hrg-6* and *hrg-4* and identify if *hrg-6* can activate or repress *hrg-4*, the *Phrg-4(3kb)::HRG-4::GFP::hrg-4* 3'UTR worm strain was generated. Confocal microscopy analysis of this strain confirmed that CeHRG-4 was localized to the apical plasma membrane of the intestine. RNAi of *hrg-6* in these transgenic worms resulted in attenuation of HRG-4::GFP expression in the intestine at low heme concentrations. Knockdown of either

*vector* or *hrg-1* did not have effect on *hrg-4* expression. These results indicate that the both *hrg-4* and *hrg-6* regulate each other at low heme (**Figure 13A & B**).

We next examined the effect of depleting *hrg-1* paralogs on worm reproduction in the RNAi-hypersensitive worm strain, VH624 (*rhIs13 V*; *nre-1(hd20)* *lin-15b (hd126)*). RNAi-hypersensitive VH624 worms were grown to the gravid adult stage on plates seeded with OP50 bacteria without additional heme. The adult P<sub>0</sub> worms were synchronized and transferred to RNAi plates grown at various heme concentrations. Live and dead progeny were counted in F<sub>1</sub> generation. Depletion of *hrg-4* at low heme concentrations resulted in a 50% reduction of live, hatched progeny when compared to worms fed vector control RNAi. No significant increase in unhatched progeny was observed when *hrg-6* was depleted. By contrast, RNAi of *hrg-4* at high heme did not have an effect on embryonic development because *hrg-4* is not expressed at this heme concentration (**Figure 14A & B**).

**Figure 1: Improved hemin utilization in yeast overexpressing CeHRG-6**

(A) Immunoblotting using an anti-HA antibody was performed on yeast transformants overexpressing C-terminal HA-tagged CeHRG-4 or CeHRG-6 in the *hem1Δ* strain. (B) Identical yeast transformants were subjected to indirect immunofluorescence microscopy to determine the intracellular localization of CeHRG-6- protein. (C) A heme-dependent growth assay was performed on *hem1Δ* yeast. Transformed yeast were grown overnight without heme, and plated in serial dilutions on medium supplemented with either 0.05 or 0.1 or 5 μM heme. (D) *hem1Δ* yeast were co- transformed with pCYC1-LacZ and either vector, CeHRG-4-HA, or CeHRG-6-HA and grown at varying heme concentrations. Cell lysates were assayed for β-galactosidase activity. (E) *hem1Δfre1Δfre2ΔMET3-FRE1* yeast were transformed with vector, CeHRG-4-HA or CeHRG-6-HA and grown with either 1 μM or 10 μM heme. Whole cells were assayed for ferric reductase activity. Error bar represent the standard error of the mean (SEM) from 3 independent experiments \*\*\* p < 0.001, \*\* p < 0.01. \* p < 0.05.

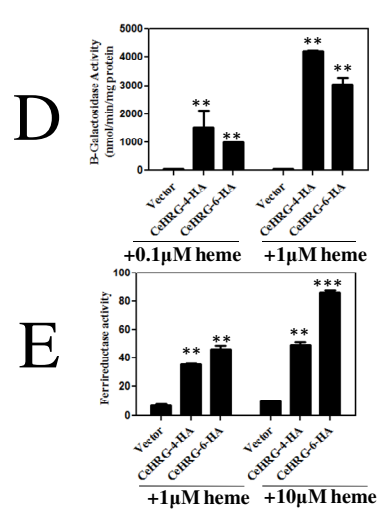
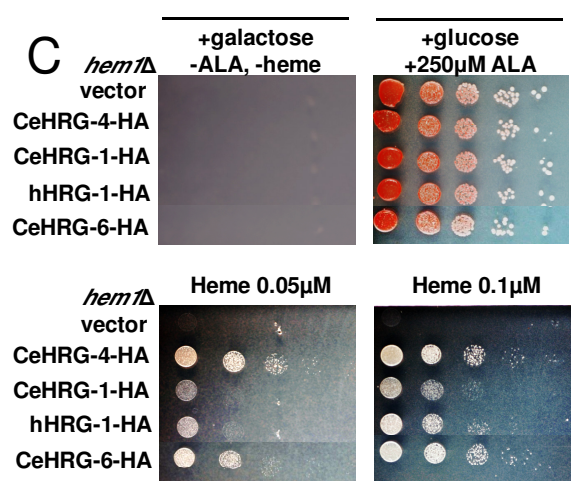
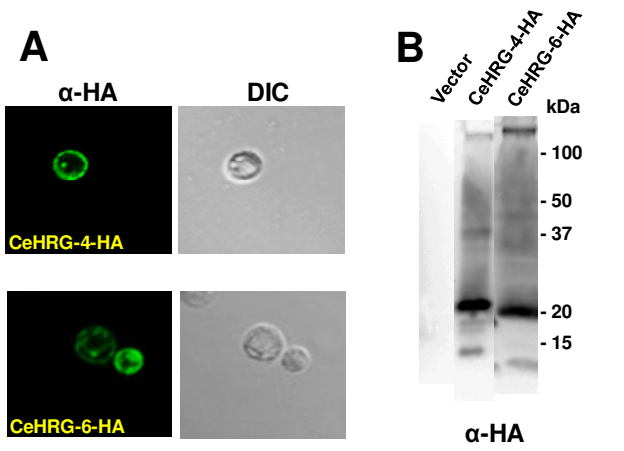


**Figure 2: Membrane Topology and Localization of CeHRG-4 and CeHRG-6.**

(A) Putative topology of CeHRG-4 and CeHRG-6 predicted by TMHMM 2.0 and SOSUI. The amino and carboxyl-termini are cytoplasmic, C1 is the cytoplasmic loop and E1 and E2 are the exoplasmic loops. Potential heme interacting residues are shaded in red. (B) CeHRG-4 and CeHRG-6 localization to the plasma membrane in mammalian cells. HEK293 cells were seeded on glass cover slips and transfected with GFP-tagged CeHRG-4 or CeHRG-6 using FuGENE 6.

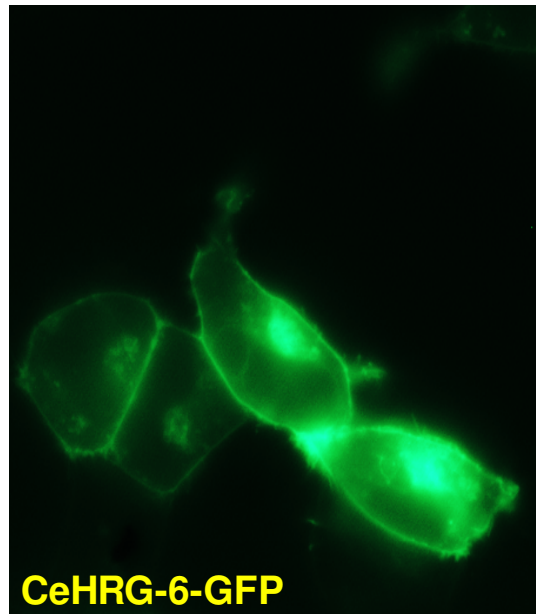
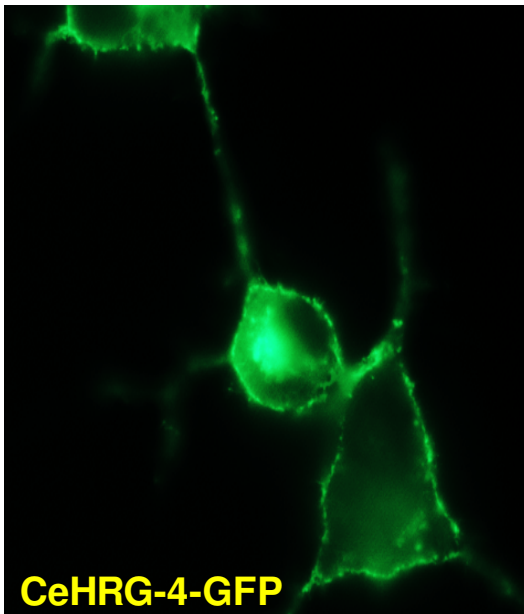
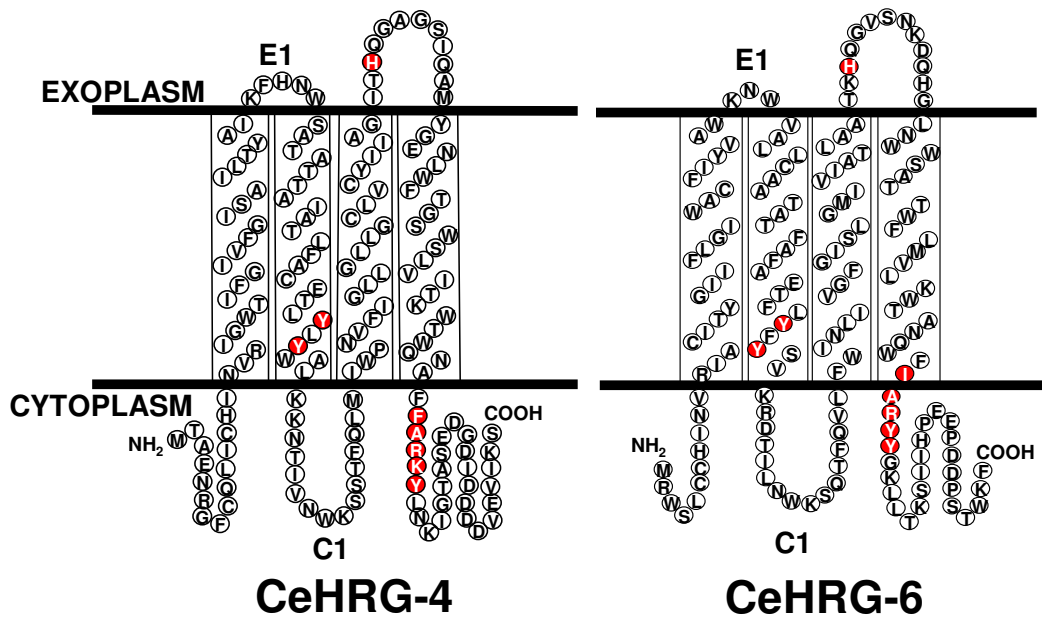


**Figure 3: Schematic representing *hrg-6* transcriptional fusion constructs.**

A) Transgenic worms were generated expressing GFP from the 1.6 kb promoter upstream of *hrg-6* transcriptional start site fused to GFP and the *hrg-6* 3' UTR. The promoter includes intergenic region between *hrg-4* and *hrg-6*. (B) Transgenic worms strain were generated using 3kb promoter upstream of the *hrg-6* transcriptional start site fused to GFP and the *hrg-6* 3' UTR. This construct included the *hrg-4* ORF located upstream of *hrg-6*, which is found in the opposite orientation on the chromosome and shown in blue. (C) A third construct was generated which contained the 3 kb promoter (including the *hrg-4* ORF) driving expression of *hrg-6* (including introns) fused to GFP and the *hrg-6* 3' UTR. An SL2 intercistronic sequence separates the *hrg-6* ORF and the GFP ORF, causing them to be translated from distinct transcripts.

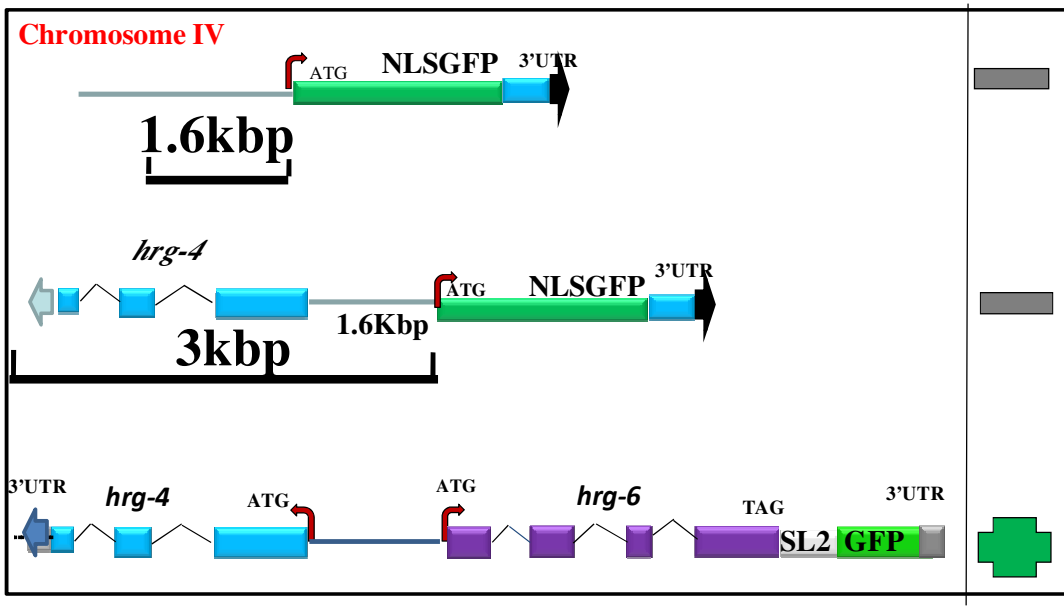
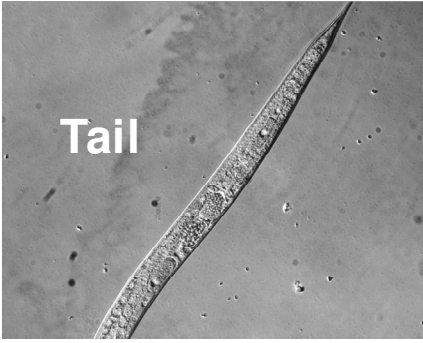
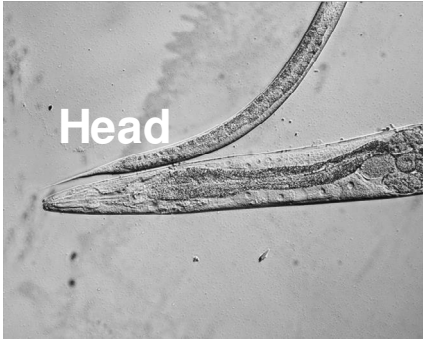


**Figure 4: Transgenic worms expressing the *Phrg-6(3kb)::HRG-6 SL2::GFP::hrg-6* 3'UTR construct express GFP in the intestine.**

This construct was generated which contained the 3 kb promoter (including the *hrg-4* ORF) driving expression of *hrg-6* (including introns) fused to GFP and the *hrg-6* 3' UTR. This construct was then transformed into the worm by microparticle bombardment. The worms were exposed to OP50 bacteria grown on NGM plates and imaged using an inverted microscope.



**DIC**



**GFP**

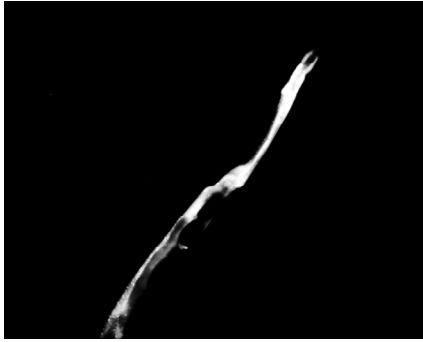
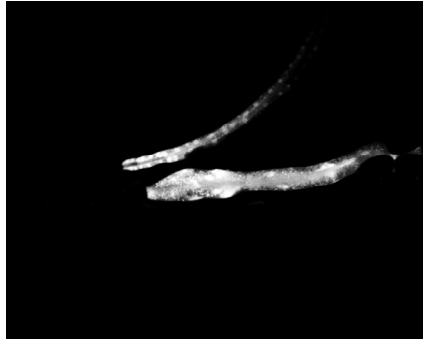


**Figure 5: Localization of HRG-6 in the intestinal cells of *C. elegans***

(A) Transgenic worms expressing the *Phrg-6*(1.6Kb)::HRG-6::GFP::*hrg-6* 3'UTR construct express mainly in the anterior intestinal cells. The 1.6 kb intergenic region of the *hrg-6* promoter or *Vha6* promoter, HRG-6::GFP, and the *hrg-6* 3'UTR were cloned by recombination into entry vectors pDONR-P4-P1R, pDONR-221 and pDONR-P2R-P3, respectively, using the Gateway BP Clonase kit. The three entry clones were then recombined into a single destination vector, pDEST-R4-R3, using the Gateway LR Clonase II Plus enzyme kit. (B) Transgenic worms expressing the *vha6* promoter::HRG-6::GFP::*unc54* 3'UTR construct express on the apical surface of the intestinal cells. These constructs were then transformed into the worm by microparticle bombardment. The worms were exposed to OP50 bacteria grown on NGM plates and imaged using an inverted microscope.

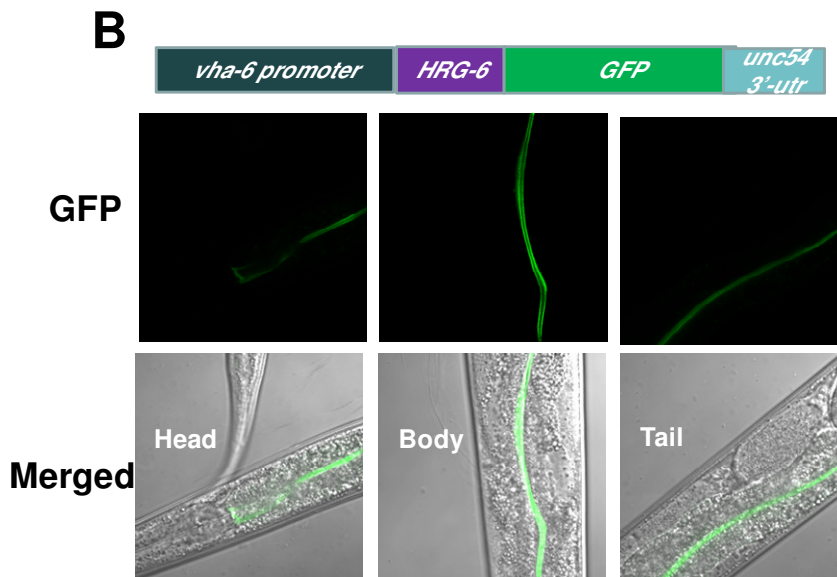
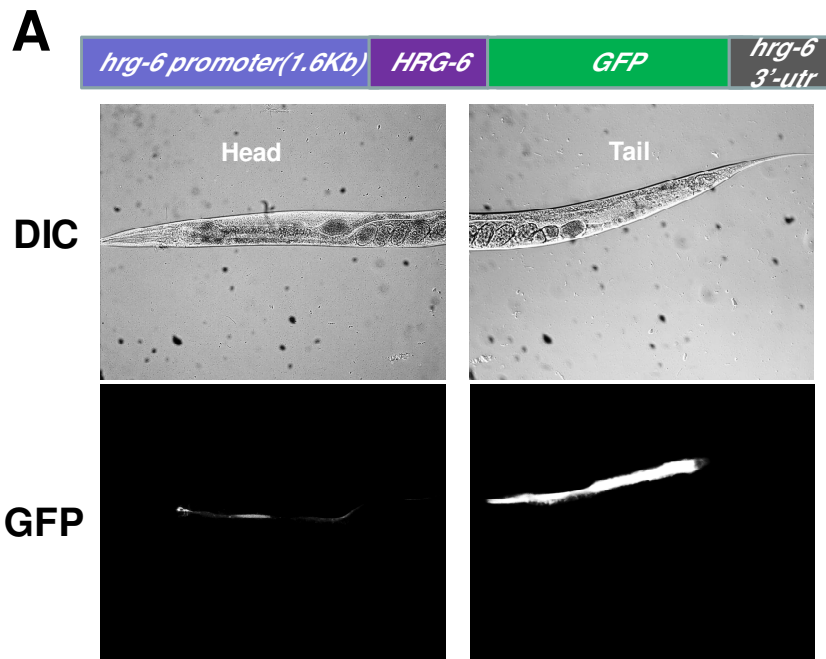


**Figure 6: *Phrg-6(3Kb)::HRG-6::GFP::hrg-6 3'UTR* transgenic worms express HRG-6 on the apical surface of worm's intestine ,uterus, and spermathecal valve of young gravid larval stage.**

HRG-6 fused to GFP and cloned into an entry vector pDONR-221 using the MultiSite Gateway system (Invitrogen). 3 kb upstream sequences of *hrg-6* promoter and the *hrg-6* 3'UTR were cloned by recombination into entry vectors pDONR-P4-P1R, and pDONRP2R- P3, respectively, using the Gateway BP Clonase kit. The three entry clones were then recombined into a single destination vector, pDEST-R4-R3, using the Gateway LR Clonase II Plus enzyme kit. This construct was then transformed into the worm by microparticle bombardment. (A) HRG-6::GFP is localized to the apical membrane of the intestine. (B) LEFT – HRG-6::GFP under control of the 3 kb promoter is expressed in the uterus (white arrow) of young adlt worms. RIGHT – HRG-6::GFP under control of the same promoter is also expressed in the spermathecal valve (white arrow) of young adult worms.

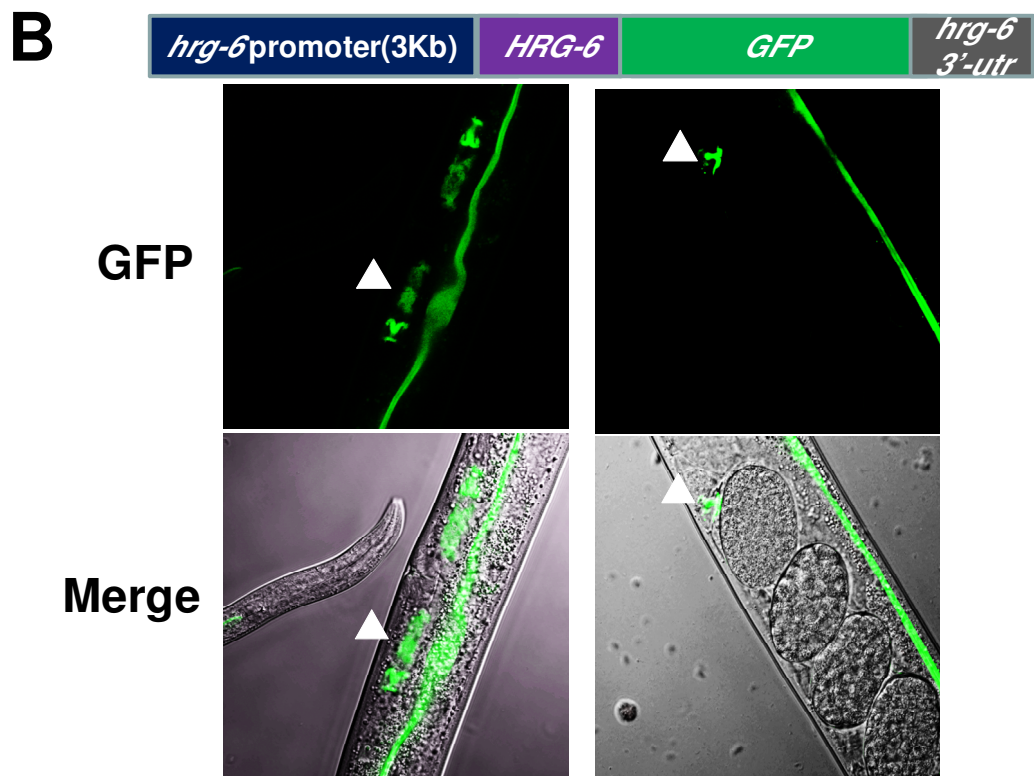
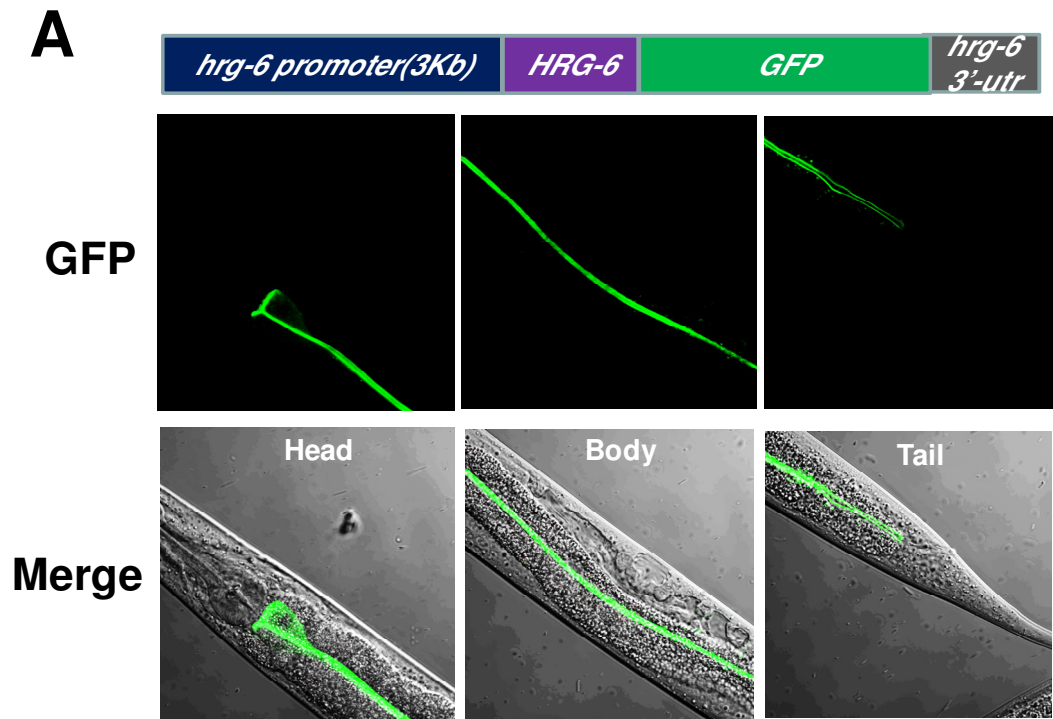


**Figure 7: *Phrg-6(3Kb)::HRG-6::GFP::unc54* 3'UTR transgenic worms express HRG-6 on the apical surface of worm's intestine ,uterus, and spermathecal valve of young gravid larval stage.**

HRG-6 fused to GFP and cloned into an entry vector pDONR-221 using the MultiSite Gateway system (Invitrogen). 3 kb upstream sequences of *hrg-6* promoter and the *unc54* 3'UTR were cloned by recombination into entry vectors pDONR-P4-P1R, and pDONRP2R- P3, respectively, using the Gateway BP Clonase kit. The three entry clones were then recombined into a single destination vector, pDEST-R4-R3, using the Gateway LR Clonase II Plus enzyme kit. This construct was then transformed into the worm by microparticle bombardment. Middle - HRG-6::GFP under control of the 3 kb promoter and generic 3'utr is expressed in the uterus (white arrow) of young adult worms. RIGHT – HRG-6::GFP under control of the same promoter is also expressed in the spermathecal valve (white arrow) of young adult worms.

*hrg-6 promoter(3Kb)* *HRG-6* *GFP* *unc54 3'-utr*

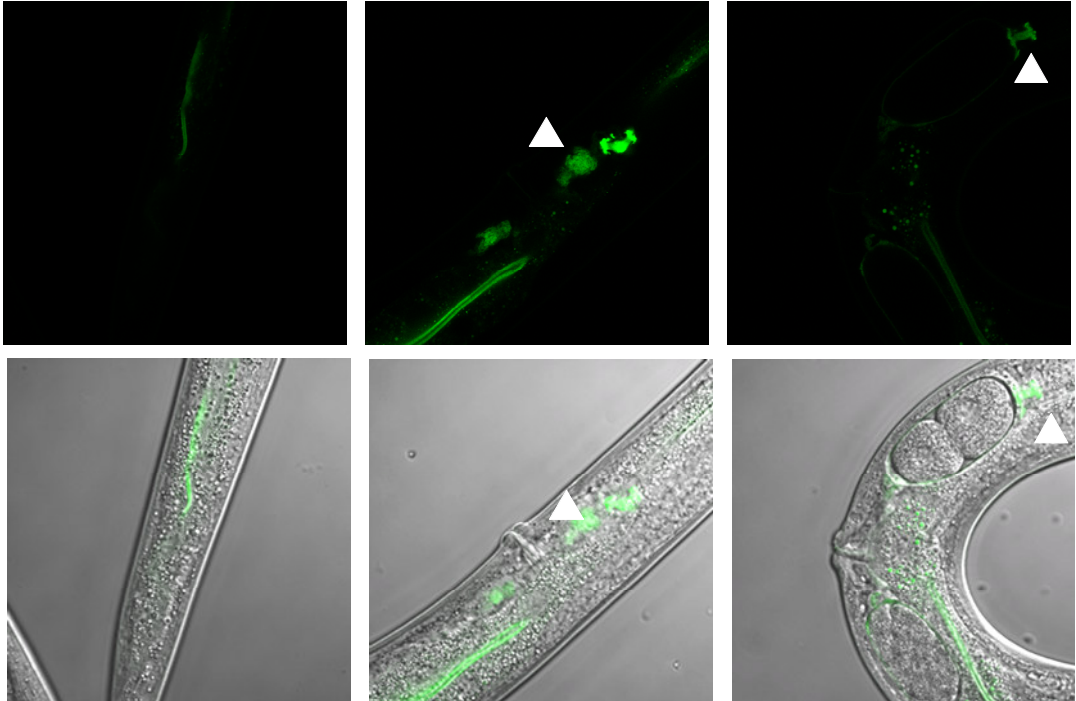
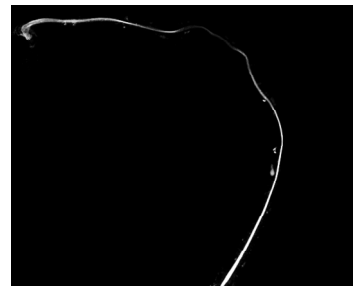
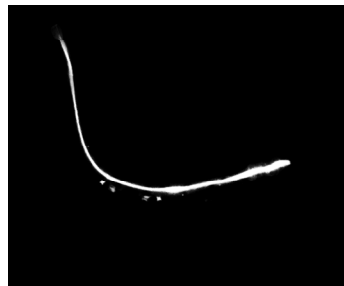


**Figure 8: Expression of HRG6::GFP is not regulated by heme.**

Worms expressing the HRG-6::GFP translational fusion show GFP expression across varying heme concentrations. The worms were initially maintained on nematode growth medium (NGM) agar plates seeded with OP50 bacteria at 20°C. Synchronized L1 larvae were then fed heme-deficient *E.coli* (RP523) grown in the presence of 4, 20, or 50  $\mu$ M heme, and the expression was analyzed by microscopy. DIC and GFP images are 20x.



**4μM heme**

**20μM heme**

**50μM heme**

**Figure 9: Transgenic worms expressing HRG-6::GFP from the 3 kb promoter containing the entire *hrg-4* locus show heme-dependent growth arrest.**

HRG-6::GFP reporter worms and wild type N2 worms were initially maintained on nematode growth medium (NGM) agar plates seeded with OP50 bacteria at 20°C. (A) Synchronized L1 larvae were then fed heme deficient *E. Coli* RP523 strain grown in 4, and 20  $\mu$ M heme and the growth was analyzed under microscope. (B) Arrested HRG-6::GFP worms grown at 4  $\mu$ M heme that were transferred to 20  $\mu$ M heme were able to develop to adult gravid stage. DIC and GFP images are 20x

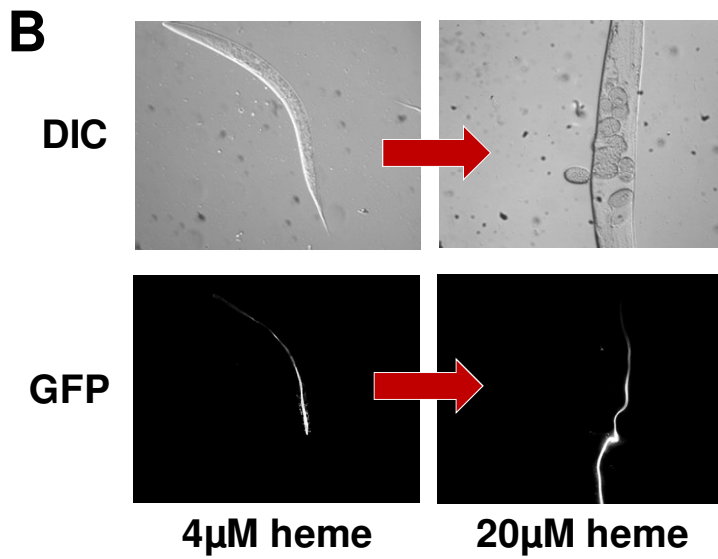
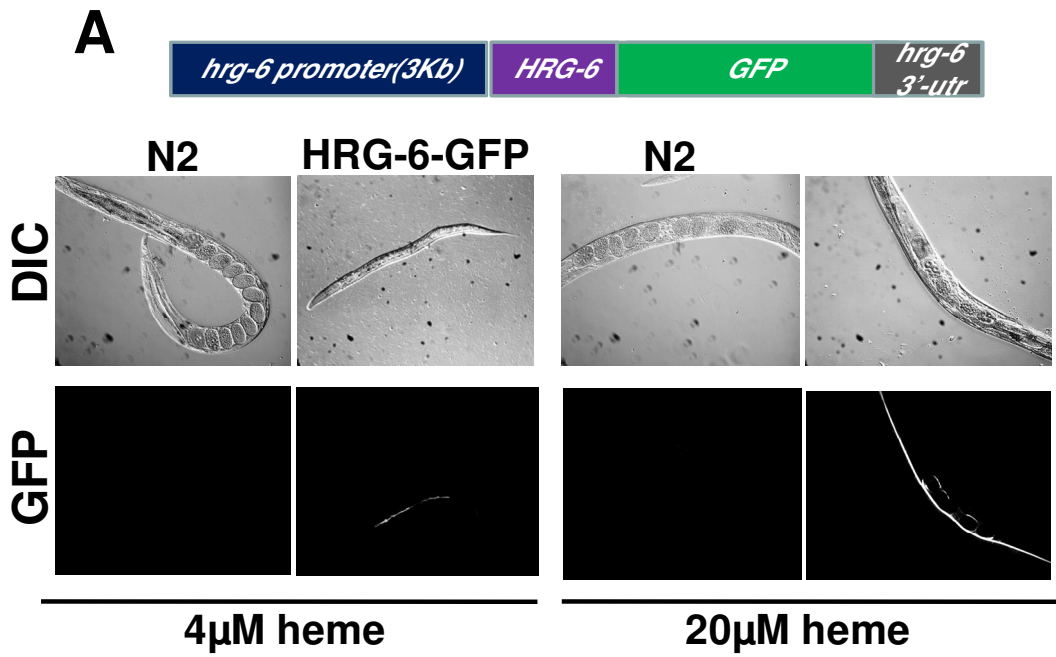
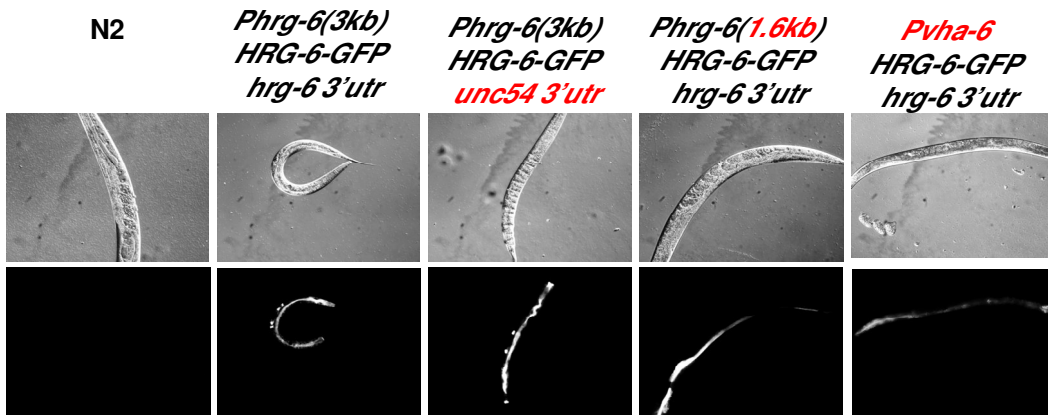


**Figure 10: Growth arrest of HRG 6::GFP worms at 4  $\mu$ M heme.**

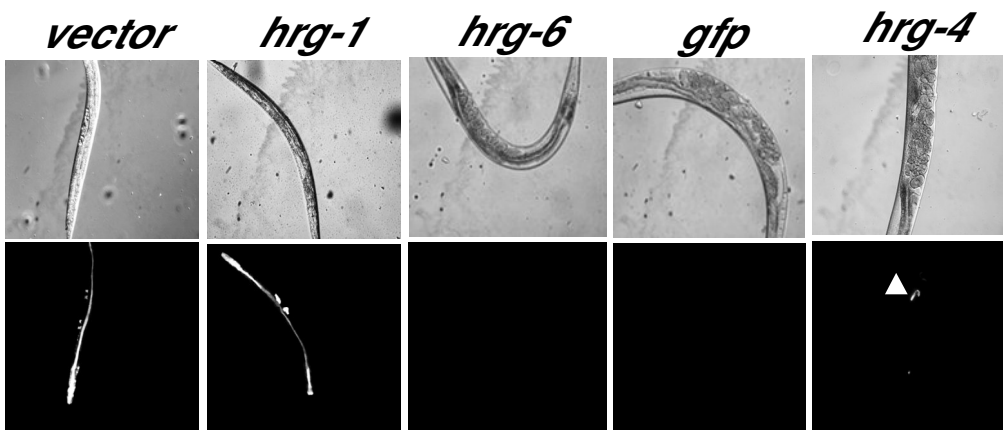
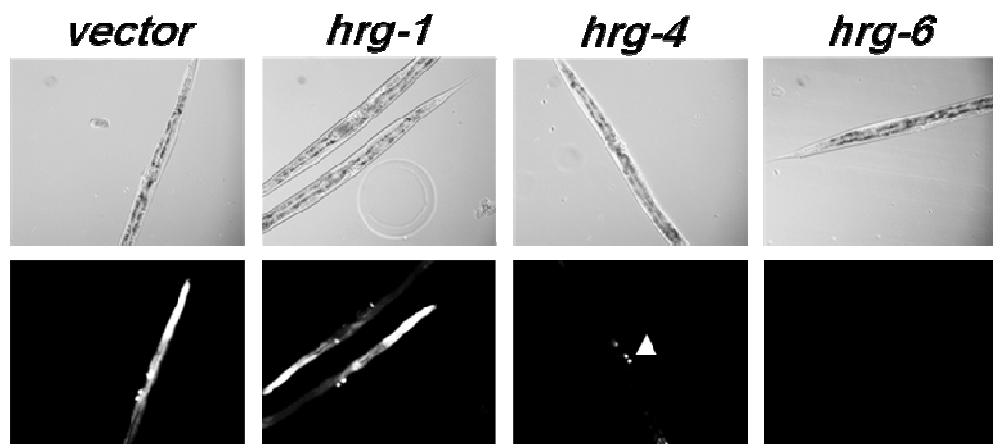
Transgenic worms were initially maintained on nematode growth medium (NGM) agar plates seeded with OP50 bacteria at 20°C. Synchronized L1 larvae were then fed heme-deficient RP523 bacteria grown in the presence of 4  $\mu$ M heme and the growth was analyzed. DIC and GFP images are 20x. Growth arrest was observed for only *Phrg-6(3Kb)::HRG-6::GFP::hrg-3'UTR* and *Phrg-6(3Kb)::HRG-6::GFP::unc543'UTR*. Both HRG-6::GFP with 1.6kb upstream sequence and with an intestinal specific *vha-6* promoter showed a slight growth delay comparing to wild type worms, but no growth arrest as observed in worms with 3kb upstream sequence.



4μM heme

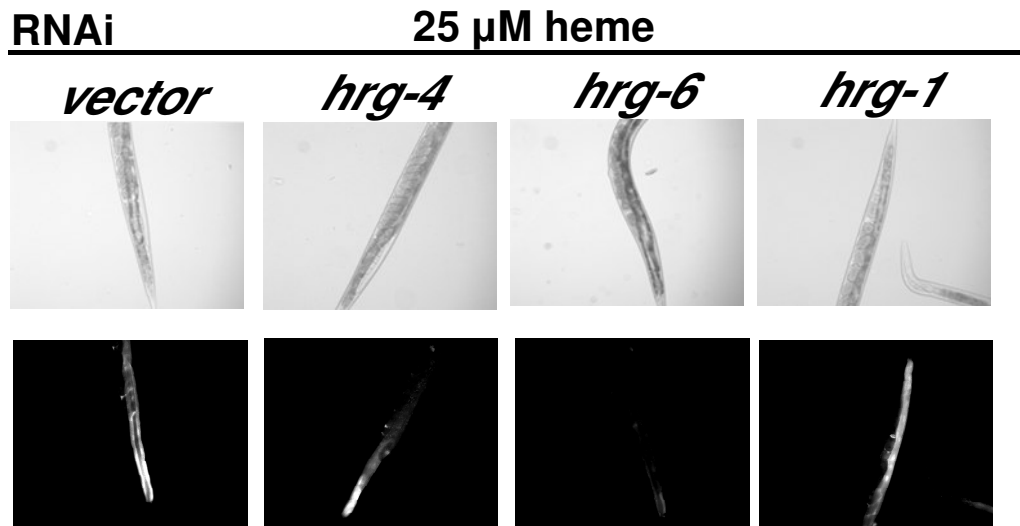
**Figure 11: The growth arrest of HRG-6::GFP transgenic worms may be due to *hrg-6* overexpression.**

(A) HRG-6 GFP Transgenic worms were initially maintained on nematode growth medium (NGM) agar plates seeded with OP50 bacteria at 20°C. Synchronized L1 larvae were then exposed to HT115 (DE3) bacteria grown in the absence of heme and induced to produce double stranded RNA against either *vector*, *hrg-1*, *hrg-4*, *hrg-6*, or *gfp*. GFP expression and growth were analyzed after 72 h by microscopy. DIC and GFP images are 20x. (A) Knockdown of *hrg-6*, *gfp* or *hrg-4* can rescue the growth arrest phenotype. The white arrow indicates spermathecal valve expression in the presence of *hrg-4* RNAi. (B) RNAi depletion of *hrg-4* reduces HRG-6::ICS::GFP expression in the worm intestine.

**A****RNAi****0  $\mu$ M heme****B****RNAi****0  $\mu$ M heme**

**Figure 12: RNAi of *hrg-4* at high heme conditions did not have an effect of GFP expression in HRG-6 GFP worm strain.**

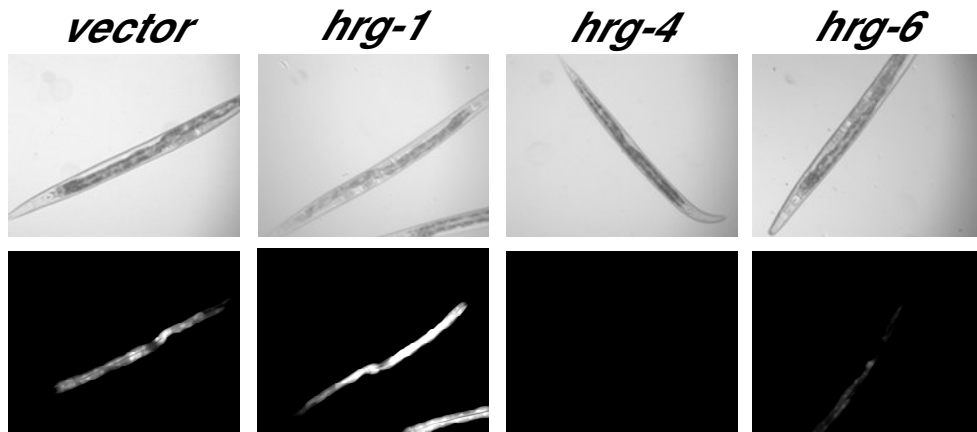
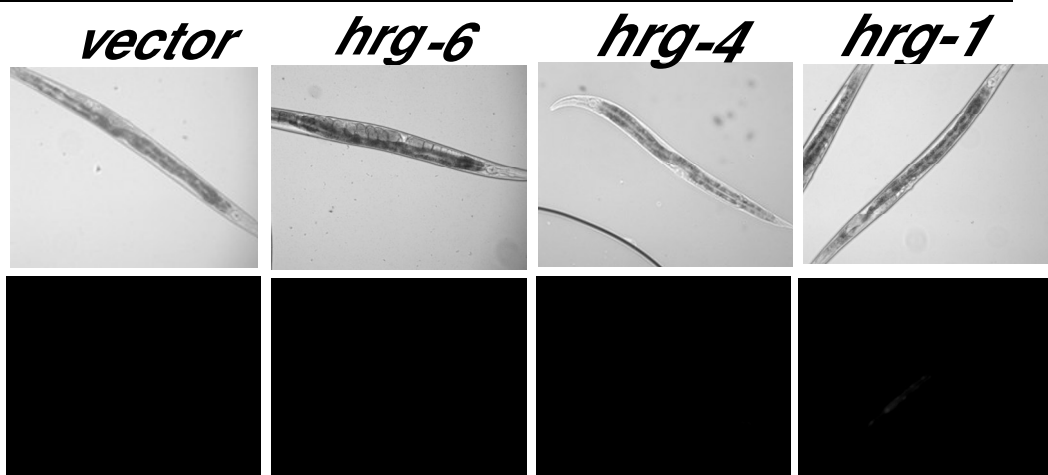
Transgenic worms were initially maintained on nematode growth medium (NGM) agar plates seeded with OP50 bacteria at 20°C. Synchronized L1 larvae were then exposed to HT115(DE3) bacteria grown in the presence 25 µM heme and induced to produce double stranded RNA against either *vector*, *hrg-1*, *hrg-4*, or *hrg-6*. GFP expression and growth were analyzed after 72 h by microscopy. DIC and GFP images are 20x.



**Figure 13: RNAi of *hrg-6* in results in attenuation of HRG-4::GFP expression in the intestine at low heme concentrations.**

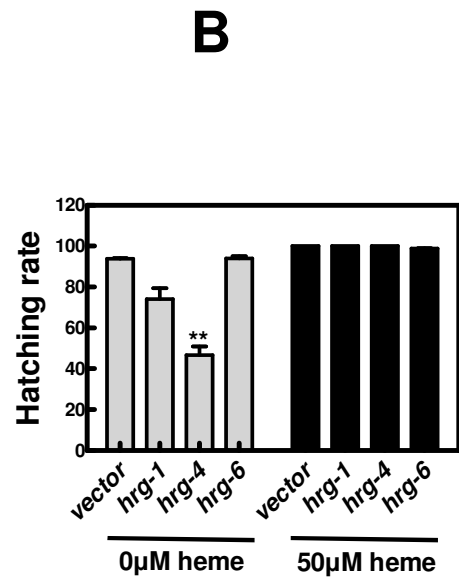
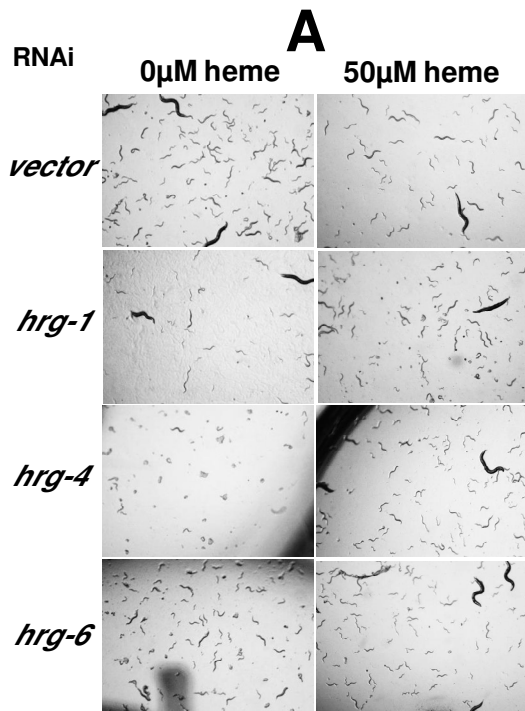
Transgenic worms were initially maintained on nematode growth medium (NGM) agar plates seeded with OP50 bacteria at 20°C. (A) Synchronized L1 larvae were then exposed to HT115 (DE3) bacteria grown in the absence of heme and induced to produce double stranded RNA against vector, *hrg-1*, *hrg-4*, or *hrg-6*.

(B) Synchronized L1 larvae were then exposed to HT115 (DE3) bacteria grown in the presence of 25µM heme and induced to produce double stranded RNA against either *vector*, *hrg-1*, *hrg-4*, or *hrg-6*. GFP expression was analyzed after 72 h by microscopy. DIC and GFP images are 20x.

**A****RNAi****0  $\mu$ M heme****B****RNAi****25  $\mu$ M heme**

**Figure 14: Depletion of *hrg-4* but not *hrg-6* in RNAi-hypersensitive worms results in decreased live progeny when worms are grown at low heme.**

The transgenic worms were initially maintained on nematode growth medium (NGM) agar plates seeded with OP50 bacteria at 20°C. Synchronized L1 larvae were then exposed to HT115 (DE3) bacteria grown in the absence of supplemented heme or presence of 50µM heme and induced to produce double stranded RNA against vector, *hrg-1*, *hrg-4*, or *hrg-6*. (A) Hatched and unhatched progeny images were taken to larvae were exposed to HT115 (DE3) bacteria grown in the absence of supplemented heme or presence of 50 µM heme. (B) Hatching rate of three gravid adults in each *hrg-1* paralog RNAi plate that exposed to HT115 (DE3) bacteria grown in the absence of supplemented heme or presence of 50 µM heme. The number of hatched and unhatched progeny was counted after 72 h.



## Chapter 4: Discussion

Heme is an essential cofactor for various biological processes. Although the synthesis and degradation of heme have been extensively studied, the mechanisms responsible for inter- and intra- cellular heme transport remain poorly understood. Utilizing *C.elegans*, we identified HRG-1 as the first eukaryotic heme importer/transporter. *C. elegans* has three additional putative paralogs of *hrg-1*, which we termed *hrg-4*, *hrg-5*, and *hrg-6*. While detailed studies have been conducted to characterize the role of CeHRG-1 and CeHRG-4 in mediating heme homeostasis, not much is known about the role of CeHRG-5 and CeHRG-6. Although both *hrg-1* and *hrg-4* are highly regulated by heme, microarray and qRT PCR analysis indicate that *hrg-5* and *hrg-6* are not heme responsive. In this study, we suggest that multiple HRG-1 paralogs (CeHRG-4, CeHRG-6) may play overlapping roles or function together to ensure heme homeostasis under varying heme conditions.

The differences in regulation of individual *hrgs* could provide molecular insights into the functional aspects of these *hrgs* and their contribution to heme homeostasis. This inference is based on the following observations: a) Depletion of *hrg-1* or *hrg-4* by RNA mediated interference in wild type worms does not result in any obvious effect on growth and development; b) *hrg-6* and *hrg-4* share the same 1.6 kb promoter region (though they are transcribed in opposite directions) and this organizational architecture is conserved in *C. elegans*, *C. briggsae* and *C. remanei*; c) the *hrg* paralogs have similar topology and conserved amino acids that have been shown to be important for heme transport; d) Both CeHRG-4 and CeHRG-6 are localized to the apical surface of the intestine and the plasma membrane in yeast and

mammalian cells; e) Our genetic studies in worms reveal that *Δhrg-1 Δhrg-4* double mutant worms show a mild growth delay only when grown under low heme conditions. We reasoned that the other HRG-1 paralogs might be providing the compensatory mechanisms for heme uptake in the worms that lack *hrg-1* and *hrg-4*.

It is difficult to understand the role of each individual paralog in *C. elegans* heme homeostasis. To overcome this issue, we have used the *hem1Δ* yeast strain which is unable to synthesize heme and lacks the ability to utilize exogenous heme at low concentrations. In the current study, we used three independent functional assays in yeast to determine the molecular characteristics of HRG-1-related proteins [59]. Functional assays in *S. cerevisiae* reveal that like CeHRG-1 and CeHRG-4, CeHRG-6 enhances the heme-dependent growth of *hem1Δ* yeast and is therefore a *potential heme* transporter. We attribute the strong ability of CeHRG-6 to rescue the growth of *hem1Δ* yeast to its plasma membrane localization; like CeHRG-4, it has greater access to extracellular heme than CeHRG-1, which is primarily localized to vacuolar membranes within the yeast cell.

The highly conserved amino acid sequences and the similar predicted topologies of these proteins hint that the mechanistic model for heme import across membranes by CeHRG-6 may be similar to that of CeHRG-4. In 2012, Yuan *et al* identified highly conserved residues that are critical for CeHRG-4-mediated heme transport, including an invariant tyrosine in the second transmembrane domain (TMD2), a histidine in the second exoplasmic loop (E2 loop) and the FARKY motif [31]. As CeHRG-4 localizes to the apical plasma membrane of the intestine, it is more likely to encounter heme in an oxidized form. Tyrosine stabilizes heme and prevents

it from carrying out oxidative chemistry [63, 64]. Yuan *et al* proposed that the histidine in the E2 loop on the extracellular/luminal side binds and transfers heme to a tyrosine in TMD2 within the channel. The heme is subsequently translocated to the cytoplasmic side, a process that is facilitated by the FARKY motif in the C-terminal tail. The aromatic and positively charged amino acids in this motif may serve as heme ligands and stabilize or orient the vinyl and propionic acid side chains [51]. Many of these residues, including the tyrosine in TMD2 and a variant of FARKY motif, LARYY in CeHRG-6, are preserved in CeHRG-6.

The ability of excess heme to rescue the defect associated with HRG-6 GFP reporter worms that were grown at low heme, as well as the fact that RNAi depletion of both *hrg-6* and GFP increases their survival, indicated that CeHRG-6 may not be required for heme import under low heme conditions. When HRG-6GFP worms are placed as L1 larvae into low heme conditions (1-4 $\mu$ M), they arrested as early L4 larvae. However, when these worms are placed at an intermediate heme concentration (20-50 $\mu$ M), they are able to develop to the adult stage. In order to successfully propagate this strain after being grown in the presence of low heme concentrations, these worms must be grown on bacteria supplemented with  $\geq 20$   $\mu$ M heme. We suggest three possibilities to explain why overexpression of *hrg-6* causes growth arrest: 1) Overexpression of *hrg-6* at low heme inhibits both endogenous and ectopically-expressed *hrg-4* at the promoter level by competing for transcriptional machinery in their shared promoters (promoter compatibility); 2) Overexpression of CeHRG-6 at low heme inhibits the function of CeHRG-4 at the protein level; and 3) As worms expressing HRG-6 GFP from the 3 kb upstream promoter region exhibit

extraintestinal expression, it is possible that *hrg-6* expression specifically in these tissues interferes with intestinal heme transport.

RNAi depletion of CeHRG-6 at low heme decreased GFP expression of CeHRG-4 worms. These data suggest that CeHRG-6 is functioning in relation to CeHRG-4. Moreover; RNAi of CeHRG-4 but not CeHRG-6 in RNAi hypersensitive worm strains decreases live, hatched progeny at low heme conditions. This may suggest that CeHRG-6 is not the primary heme transporter in low heme conditions. It is also possible that CeHRG-6 is a regulator of CeHRG-4. Such a regulation is observed between Ctr-1 and Ctr-2. Ctr1<sup>-/-</sup> mice fail to gastrulate and die *in utero*, while Ctr2 null mice show no growth phenotypes [65, 66]. Recent work showed that Ctr-2 in fact regulates the activity of Ctr-1 by directly interacting with Ctr-1 [67].

Our studies showed plasma membrane localization for HRG-4 GFP and HRG-6 GFP in yeast, mammalian cells, and worms. When the C-terminus of CeHRG-1 was replaced with the C-terminal domain of CeHRG-4, CeHRG-114CFP was seen on the plasma membrane of HEK293 cells (**Appendix 1**). Conversely, CeHRG-441, localized to the endosomal-lysosomal membranes. FPP assays in mammalian cells revealed the C-terminal domains of HRG-1-related proteins reside in the cytoplasm. These findings indicate that the C-terminal domains of CeHRG-4 are required for proper protein localization, which we speculate must also be true for CeHRG-6.

Our previous studies showed that HRG-1-related proteins migrate as dimers and trimers on SDS/ PAGE gel in non denaturing conditions. This is raising the possibility that HRG-1-related proteins function as multimers [43]. Such a situation is observed in Ctr-family integral membrane proteins which assemble as multimers,

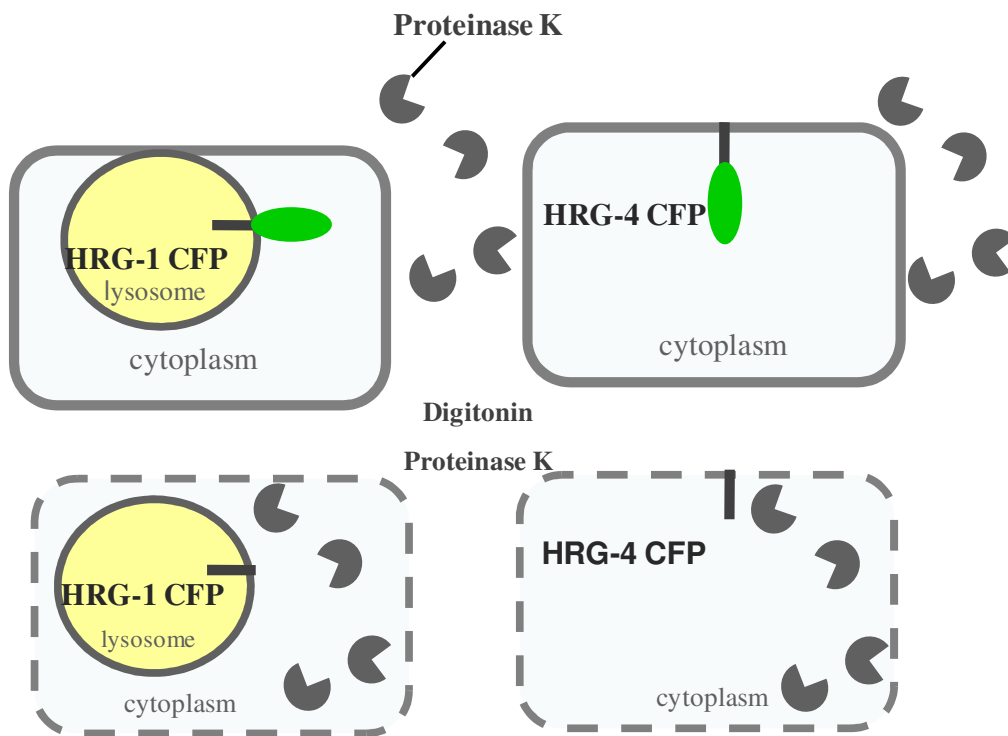
and form a channel lined with ligands for copper binding and transport [68-71]. The co-immunoprecipitation of proteins from cellular fractions will be the most convincing evidence that two or more proteins physically interact *in vivo* [72-74]. In addition to and complementary with the above, bimolecular fluorescence complementation (BiFC) assay can be used to verify if CeHRG-6 and CeHRG-4 interact with each other.

Our results indicate that CeHRG-1-related proteins are differentially regulated by heme, localized to distinct intracellular membranes and plausibly form heterotypic multimers. If true, these models of regulation will provide a diverse, multi-pronged mode of regulation for uptake of heme, an essential but toxic nutrient.

## **Appendices**

### **Appendix I: A cartoon of the FPP illustrates a single cell before and after digitonin and proteinase K treatments.**

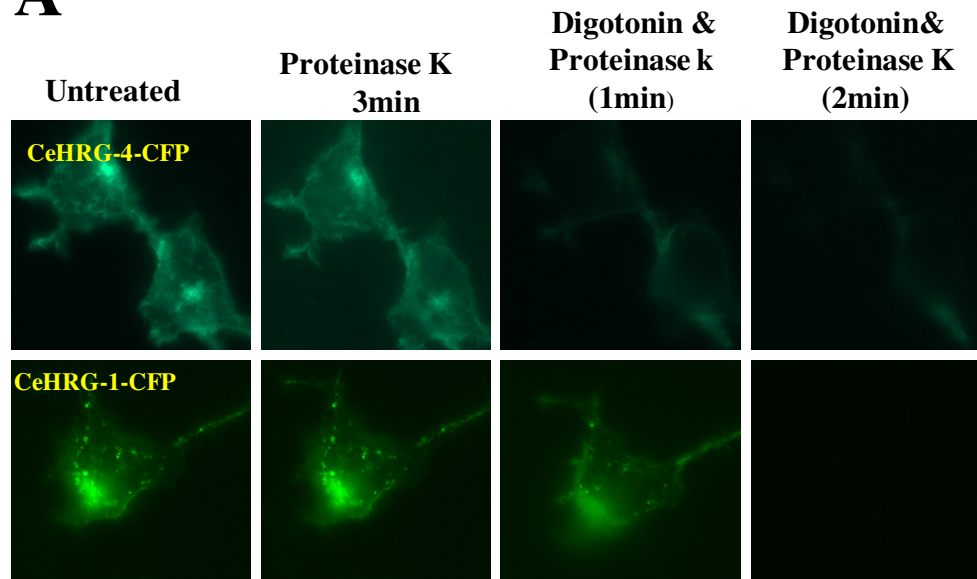
Treatment of proteinase K alone will degrade the C-terminal tag if facing the exoplasmic surface of the cell, while the intracellular GFP tags will be protected. After a brief treatment with digitonin and proteinase K, the GFP tag of CeHRG-4 was degraded, while the C-terminal tag of CeHRG-1 remained protected. After further treatment with digitonin and proteinase K, the CeHRG-1 tag was degraded, indicating that the C-terminus is located in an intracellular compartment.



**Appendix II: fluorescence protease protection assay indicates that the C-terminus of HRG-4 is located in the cytosol and the C-terminus of HRG-1 is located within an intracellular compartment.**

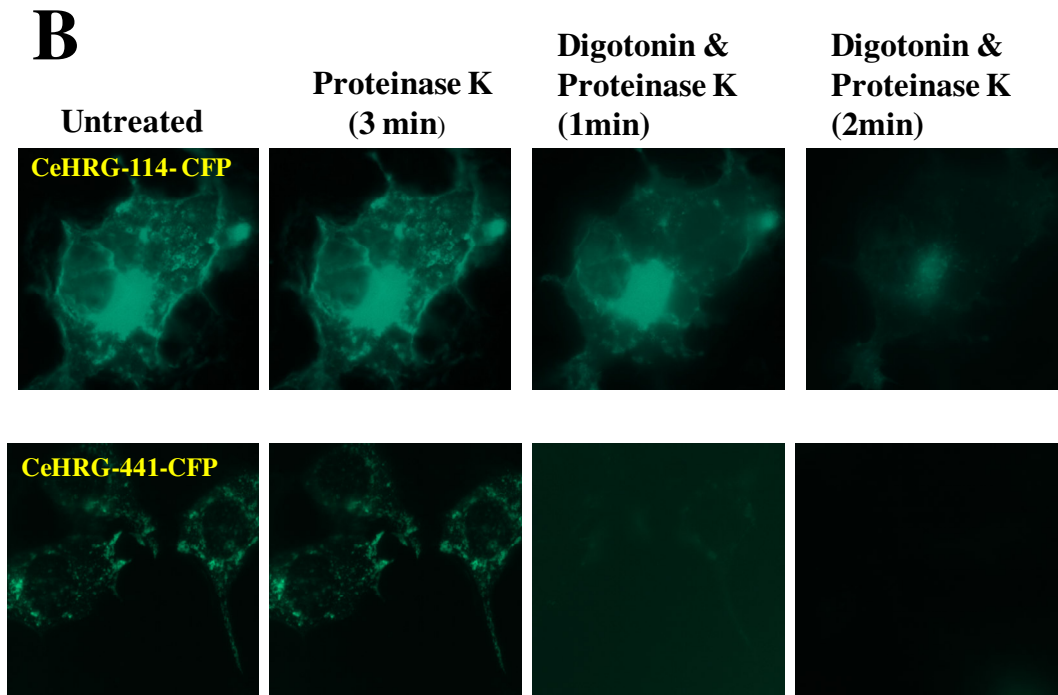
A fluorescence protease protection (FPP) assay was performed using CeHRG-1 and CeHRG-4 CFP chimeras expressed in live HEK293 cells. The assay is based on ability of proteases to degrade exposed polypeptides versus their inability to digest protected polypeptides.

**A**



**Appendix III: The C-terminal domains for both CeHRG-114-CFP and CeHRG-441-CFP are cytoplasmic and are required for proper protein localization.**

Fluorescence protease protection (FPP) assay was done by using GFP chimeras expressed in HEK293 living cells. The assay is based on ability of proteases to degrade exposed polypeptides versus their inability to digest protected polypeptides. The C-terminus of CeHRG-1 was replaced with the C-terminal domain of CeHRG-4 and named CeHRG-114CFP. The C-terminus of CeHRG-4 was replaced with the C-terminal domain of CeHRG-1 and named CeHRG-441CFP. [61].



#### Appendix IV: Reporter constructs used in this study.

Strain name	Genotype
IQ6161	1.6 Kb upstream of <i>hrg-6::hrg6-gfp::hrg-6</i> UTR
IQ6162	3 Kb upstream of <i>hrg-6::hrg6-gfp::hrg-6</i> UTR
IQ6163	3 Kb upstream of <i>hrg-6::hrg6-gfp::unc54</i> UTR
IQ6164	<i>vha6</i> promoter:: <i>hrg6-gfp::unc54</i> UTR
IQ6361	3 Kb upstream of <i>hrg-6::hrg6::SL2::gfp::hrg-6</i> UTR
IQ6362	3 Kb upstream of <i>hrg-6::hrg6flag::SL2::gfp::hrg-6</i> UTR
IQ6341	3 Kb upstream of <i>hrg4::hrg4flag::SL2::gfp::hrg-4</i> UTR
IQ6061	1.6 Kb upstream of <i>hrg-6::gfp::hrg-6</i> UTR
IQ6062	3 Kb upstream of <i>hrg-6::gfp::hrg-6</i> UTR

## Appendix V: Oligonucleotides used in this study.

Name	Sequence (5' to 3')
5'promotor 1.6kb	GGGGACAACCTTTGTATAGAAAAGTTGNACATTCAAAGATTGTAACTTAAACAATTAA
3'promotor hrg-6p	GGGGACTGCTTTTTT GTA CAAACTTGCAACATAATTATGCAAAAAACAAATAGAACT
reverse prom hrg-6#1	GGGG ACTGCTTTTTTGTACAAACTTGCTCCATCTAATATAAACCCAATAATTTTAGTTACGGT
reverse prom hrg-6#2	GGGGACTGC TTT TTT GTACAAACTTGCTGGCAGTCGACCACCAATTTAAACCAT
5'B23utr hrg-6	GGGG AC AAC TTT GTA TAA TAA AGT TGTCATGGGATAGATGTGATCATCGCG
5'B23utr hrg-6	GGGG ACA GCT TTC TTG TACAAAAGTGGCAAATGTTGATTTAGTTTTACATTTTCGTGTG
5'hrg-6-gfp	GAGCCAGATGAT CCA TCA ACT TGG AAG TTTATG AGT AAA GGA GAA GAA CTT TTC ACT
3' gfp- hrg-6	AGTGAAAAGTTC TTCTCCTTACTCAT AAACCTT CCAAGT TGATGGATCATCTGGCTC
5'attB1HRG-6	GGGGACAAGTTTGTACAAAAAAGCAGGCTAATACGCGACCAGAAACACAACGTGTATTGCA AGCT

## Bibliography:

1. Iron deficiency anaemia: assessment, prevention and control. A guide for programme managers. In., 2001 edn: Document WHO/NHD/01.3; 2001.
2. Micronutrient deficiencies. Battling iron deficiency anaemia: The challenge.. In.; 2012.
3. Akin C *et al*: Effects of tyrosine kinase inhibitor STI571 on human mast cells bearing wild-type or mutated c-kit. *Exp Hematol* 2003, 31(8):686-692.[PMID:12901973]
4. Monsen ER, Page JF: Effects of EDTA and ascorbic acid on the absorption of iron from an isolated rat intestinal loop. *J Agric Food Chem* 1978, 26(1):223-226.[PMID:413853]
5. Roughead ZK, Hunt JR: Adaptation in iron absorption: iron supplementation reduces nonheme-iron but not heme-iron absorption from food. *Am J Clin Nutr* 2000, 72(4):982-989.[PMID:11010941]
6. Heinemann IU, Jahn M, Jahn D: The biochemistry of heme biosynthesis. *Arch Biochem Biophys* 2008, 474(2):238-251.[PMID:18314007]
7. Tsiftoglou AS, Tsamadou AI, Papadopoulou LC: Heme as key regulator of major mammalian cellular functions: molecular, cellular, and pharmacological aspects. *Pharmacol Ther* 2006, 111(2):327-345.[PMID:16513178]
8. Nakajima O *et al*: Heme deficiency in erythroid lineage causes differentiation arrest and cytoplasmic iron overload. *EMBO J* 1999, 18(22):6282-6289.[PMID:10562540]
9. Ogawa K *et al*: Heme mediates derepression of Maf recognition element through direct binding to transcription repressor Bach1. *EMBO J* 2001, 20(11):2835-2843.[PMID:11387216]
10. Ponka P: Cell biology of heme. *Am J Med Sci* 1999, 318(4):241-256.[PMID:10522552]
11. Yin L *et al*: Rev-erbalpha, a heme sensor that coordinates metabolic and circadian pathways. *Science* 2007, 318(5857):1786-1789.[PMID:18006707]
12. Faller M, Matsunaga M, Yin S, Loo JA, Guo F: Heme is involved in microRNA processing. *Nat Struct Mol Biol* 2007, 14(1):23-29.[PMID:17159994]

13. Severance S, Hamza I: Trafficking of heme and porphyrins in metazoa. *Chem Rev* 2009, 109(10):4596-4616.[PMID:19764719]
14. Rao AU, Carta LK, Lesuisse E, Hamza I: Lack of heme synthesis in a free-living eukaryote. *Proc Natl Acad Sci U S A* 2005, 102(12):4270-4275.[PMID:15767563]
15. Gilleard JS: Understanding anthelmintic resistance: the need for genomics and genetics. *Int J Parasitol* 2006, 36(12):1227-1239.[PMID:16889782]
16. Ajioka RS, Phillips JD, Kushner JP: Biosynthesis of heme in mammals. *Biochim Biophys Acta* 2006, 1763(7):723-736.[PMID:16839620]
17. Shemin D, Rittenberg D: On the utilization of glycine for uric acid synthesis in man. *J Biol Chem* 1947, 167(3):875.[PMID:20287924]
18. Riddle RD, Yamamoto M, Engel JD: Expression of delta-aminolevulinate synthase in avian cells: separate genes encode erythroid-specific and nonspecific isozymes. *Proc Natl Acad Sci U S A* 1989, 86(3):792-796.[PMID:2915978]
19. Kaasik K, Lee CC: Reciprocal regulation of haem biosynthesis and the circadian clock in mammals. *Nature* 2004, 430(6998):467-471.[PMID:15269772]
20. Bevan DR, Bodlaender P, Shemin D: Mechanism of porphobilinogen synthase. Requirement of Zn<sup>2+</sup> for enzyme activity. *J Biol Chem* 1980, 255(5):2030-2035.[PMID:7354072]
21. Erskine PT *et al*: X-ray structure of 5-aminolaevulinate dehydratase, a hybrid aldolase. *Nat Struct Biol* 1997, 4(12):1025-1031.[PMID:9406553]
22. Jaffe EK: An unusual phylogenetic variation in the metal ion binding sites of porphobilinogen synthase. *Chem Biol* 2003, 10(1):25-34.[PMID:12573695]
23. Shoolingin-Jordan PM, Al-Dbass A, McNeill LA, Sarwar M, Butler D: Human porphobilinogen deaminase mutations in the investigation of the mechanism of dipyrromethane cofactor assembly and tetrapyrrole formation. *Biochem Soc Trans* 2003, 31(Pt 3):731-735.[PMID:12773194]
24. Krishnamurthy PC *et al*: Identification of a mammalian mitochondrial porphyrin transporter. *Nature* 2006, 443(7111):586-589.[PMID:17006453]
25. Grandchamp B, Phung N, Nordmann Y: The mitochondrial localization of coproporphyrinogen III oxidase. *Biochem J* 1978, 176(1):97-102.[PMID:31872]

26. Conder LH, Woodard SI, Dailey HA: Multiple mechanisms for the regulation of haem synthesis during erythroid cell differentiation. Possible role for coproporphyrinogen oxidase. *Biochem J* 1991, 275 ( Pt 2):321-326.[PMID:2025219]
27. Koch M *et al*: Crystal structure of protoporphyrinogen IX oxidase: a key enzyme in haem and chlorophyll biosynthesis. *EMBO J* 2004, 23(8):1720-1728.[PMID:15057273]
28. Dailey HA: Terminal steps of haem biosynthesis. *Biochem Soc Trans* 2002, 30(4):590-595.[PMID:12196143]
29. Zenke-Kawasaki Y *et al*: Heme induces ubiquitination and degradation of the transcription factor Bach1. *Mol Cell Biol* 2007, 27(19):6962-6971.[PMID:17682061]
30. Tahara T *et al*: Heme positively regulates the expression of beta-globin at the locus control region via the transcriptional factor Bach1 in erythroid cells. *J Biol Chem* 2004, 279(7):5480-5487.[PMID:14660636]
31. Krogh A, Larsson B, von Heijne G, Sonnhammer EL: Predicting transmembrane protein topology with a hidden Markov model: application to complete genomes. *J Mol Biol* 2001, 305(3):567-580.[PMID:11152613]
32. Lipovich L, Hughes AL, King MC, Abkowitz JL, Quigley JG: Genomic structure and evolutionary context of the human feline leukemia virus subgroup C receptor (hFLVCR) gene: evidence for block duplications and de novo gene formation within duplicons of the hFLVCR locus. *Gene* 2002, 286(2):203-213.[PMID:11943475]
33. Quigley JG *et al*: Cloning of the cellular receptor for feline leukemia virus subgroup C (FeLV-C), a retrovirus that induces red cell aplasia. *Blood* 2000, 95(3):1093-1099.[PMID:10648427]
34. Quigley JG *et al*: Identification of a human heme exporter that is essential for erythropoiesis. *Cell* 2004, 118(6):757-766.[PMID:15369674]
35. Keel SB *et al*: A heme export protein is required for red blood cell differentiation and iron homeostasis. *Science* 2008, 319(5864):825-828.[PMID:18258918]
36. Yang Z *et al*: Kinetics and specificity of feline leukemia virus subgroup C receptor (FLVCR) export function and its dependence on hemopexin. *J Biol Chem* 2010, 285(37):28874-28882.[PMID:20610401]

37. Rajadhyaksha AM *et al*: Mutations in FLVCR1 cause posterior column ataxia and retinitis pigmentosa. *Am J Hum Genet* 2010, 87(5):643-654.[PMID:21070897]
38. Ishiura H *et al*: Posterior column ataxia with retinitis pigmentosa in a Japanese family with a novel mutation in FLVCR1. *Neurogenetics* 2011, 12(2):117-121.[PMID:21267618]
39. Krishnamurthy P, Schuetz JD: The ABC transporter Abcg2/Bcrp: role in hypoxia mediated survival. *Biometals* 2005, 18(4):349-358.[PMID:16158227]
40. Jonker JW *et al*: The breast cancer resistance protein protects against a major chlorophyll-derived dietary phototoxin and protoporphyria. *Proc Natl Acad Sci U S A* 2002, 99(24):15649-15654.[PMID:12429862]
41. Krishnamurthy P *et al*: The stem cell marker Bcrp/ABCG2 enhances hypoxic cell survival through interactions with heme. *J Biol Chem* 2004, 279(23):24218-24225.[PMID:15044468]
42. Severance S *et al*: Genome-wide analysis reveals novel genes essential for heme homeostasis in *Caenorhabditis elegans*. *PLoS Genet* 2010, 6(7):e1001044.[PMID:20686661]
43. Rajagopal A *et al*: Haem homeostasis is regulated by the conserved and concerted functions of HRG-1 proteins. *Nature* 2008, 453(7198):1127-1131.[PMID:18418376]
44. Hentze MW, Muckenthaler MU, Galy B, Camaschella C: Two to tango: regulation of Mammalian iron metabolism. *Cell* 2010, 142(1):24-38.[PMID:20603012]
45. Schultz IJ, Chen C, Paw BH, Hamza I: Iron and porphyrin trafficking in heme biogenesis. *J Biol Chem* 2010, 285(35):26753-26759.[PMID:20522548]
46. Shayeghi M *et al*: Identification of an intestinal heme transporter. *Cell* 2005, 122(5):789-801.[PMID:16143108]
47. Le Blanc S, Garrick MD, Arredondo M: Heme carrier protein 1 transports heme and is involved in heme-Fe metabolism. *Am J Physiol Cell Physiol* 2012, 302(12):C1780-1785.[PMID:22496243]
48. Duffy SP *et al*: The Fowler syndrome-associated protein FLVCR2 is an importer of heme. *Mol Cell Biol* 2010, 30(22):5318-5324.[PMID:20823265]

49. Brown JK, Fung C, Tailor CS: Comprehensive mapping of receptor-functioning domains in feline leukemia virus subgroup C receptor FLVCR1. *J Virol* 2006, 80(4):1742-1751.[PMID:16439531]
50. White C *et al*: HRG1 is essential for heme transport from the phagolysosome of macrophages during erythrophagocytosis. *Cell Metab* 2013, 17(2):261-270.[PMID:23395172]
51. Yuan X, Protchenko O, Philpott CC, Hamza I: Topologically conserved residues direct heme transport in HRG-1-related proteins. *J Biol Chem* 2012, 287(7):4914-4924.[PMID:22174408]
52. Ito H, Fukuda Y, Murata K, Kimura A: Transformation of intact yeast cells treated with alkali cations. *J Bacteriol* 1983, 153(1):163-168.[PMID:6336730]
53. Adams DE, Gottschling CA, Kaiser T: *Methods in yeast genetics*: Cold Spring Harbor Press; 2000.
54. Dancis A, Klausner RD, Hinnebusch AG, Barriocanal JG: Genetic evidence that ferric reductase is required for iron uptake in *Saccharomyces cerevisiae*. *Mol Cell Biol* 1990, 10(5):2294-2301.[PMID:2183029]
55. Ahringer J: The *C. elegans* Research Community. In.: *WormBook*, ed; (2006) (*WormBook*, ed), .: *WormBook*, doi/10.1895/wormbook.1891.1847.1891.
56. Praitis V, Casey E, Collar D, Austin J: Creation of low-copy integrated transgenic lines in *Caenorhabditis elegans*. *Genetics* 2001, 157(3):1217-1226.[PMID:11238406]
57. Li JM, Umanoff H, Proenca R, Russell CS, Cosloy SD: Cloning of the *Escherichia coli* K-12 hemB gene. *J Bacteriol* 1988, 170(2):1021-1025.[PMID:3276659]
58. Lorenz H, Hailey DW, Lippincott-Schwartz J: Fluorescence protease protection of GFP chimeras to reveal protein topology and subcellular localization. *Nat Methods* 2006, 3(3):205-210.[PMID:16489338]
59. Protchenko O *et al*: Role of PUG1 in inducible porphyrin and heme transport in *Saccharomyces cerevisiae*. *Eukaryot Cell* 2008, 7(5):859-871.[PMID:18326586]
60. Protchenko O, Rodriguez-Suarez R, Androphy R, Bussey H, Philpott CC: A screen for genes of heme uptake identifies the FLC family required for import of FAD into the endoplasmic reticulum. *J Biol Chem* 2006, 281(30):21445-21457.[PMID:16717099]
61. Zhang L, Hach A: Molecular mechanism of heme signaling in yeast: the transcriptional activator Hap1 serves as the key mediator. *Cell Mol Life Sci* 1999, 56(5-6):415-426.[PMID:11212295]

62. Blumenthal T *et al*: A global analysis of *Caenorhabditis elegans* operons. *Nature* 2002, 417(6891):851-854.[PMID:12075352]
63. Goodwin DC, Rowlinson SW, Marnett LJ: Substitution of tyrosine for the proximal histidine ligand to the heme of prostaglandin endoperoxide synthase 2: implications for the mechanism of cyclooxygenase activation and catalysis. *Biochemistry* 2000, 39(18):5422-5432.[PMID:10820014]
64. Liu Y *et al*: Replacement of the proximal histidine iron ligand by a cysteine or tyrosine converts heme oxygenase to an oxidase. *Biochemistry* 1999, 38(12):3733-3743.[PMID:10090762]
65. Kuo YM, Zhou B, Cosco D, Gitschier J: The copper transporter CTR1 provides an essential function in mammalian embryonic development. *Proc Natl Acad Sci U S A* 2001, 98(12):6836-6841.[PMID:11391004]
66. Lee J, Prohaska JR, Thiele DJ: Essential role for mammalian copper transporter Ctr1 in copper homeostasis and embryonic development. *Proc Natl Acad Sci U S A* 2001, 98(12):6842-6847.[PMID:11391005]
67. Ohrvik H *et al*: Ctr2 regulates biogenesis of a cleaved form of mammalian Ctr1 metal transporter lacking the copper- and cisplatin-binding ecto-domain. *Proc Natl Acad Sci U S A* 2013, 110(46):E4279-4288.[PMID:24167251]
68. Pena MM, Puig S, Thiele DJ: Characterization of the *Saccharomyces cerevisiae* high affinity copper transporter Ctr3. *J Biol Chem* 2000, 275(43):33244-33251.[PMID:10924521]
69. Dancis A, Haile D, Yuan DS, Klausner RD: The *Saccharomyces cerevisiae* copper transport protein (Ctr1p). Biochemical characterization, regulation by copper, and physiologic role in copper uptake. *J Biol Chem* 1994, 269(41):25660-25667.[PMID:7929270]
70. Lee J, Pena MM, Nose Y, Thiele DJ: Biochemical characterization of the human copper transporter Ctr1. *J Biol Chem* 2002, 277(6):4380-4387.[PMID:11734551]
71. De Feo CJ, Aller SG, Siluvai GS, Blackburn NJ, Unger VM: Three-dimensional structure of the human copper transporter hCTR1. *Proc Natl Acad Sci U S A* 2009, 106(11):4237-4242.[PMID:19240214]
72. Dandekar T, Snel B, Huynen M, Bork P: Conservation of gene order: a fingerprint of proteins that physically interact. *Trends Biochem Sci* 1998, 23(9):324-328.[PMID:9787636]

73. Monti M, Orru S, Pagnozzi D, Pucci P: Interaction proteomics. *Biosci Rep* 2005, 25(1-2):45-56.[PMID:16222419]
74. Phee BK *et al*: Identification of phytochrome-interacting protein candidates in *Arabidopsis thaliana* by co-immunoprecipitation coupled with MALDI-TOF MS. *Proteomics* 2006, 6(12):3671-3680.[PMID:16705748]